Role of IgM and IgA Antibodies in the Neutralization of SARS-CoV-2

Jéromine Klingler[1,2], Svenja Weiss[1,2], Vincenza Itri[1], Xiaomei Liu[1,2], Kasopefoluwa Y. Oguntuyo[3], Christian Stevens[3], Satoshi Ikegame[3], Chuan-Tien Hung[3], Gospel Enyindah-Asonye[1], Fatima Amanat[3,4], Ian Baine[5], Suzanne Arinsburg[5], Juan C. Bandres[2], Erna Milunka Kojic[6], Jonathan Stoever[7], Denise Jurczyszak[3,4], Maria Bermudez-Gonzalez[3], Viviana Simon[1,3,8], Arthur Nádas[9], Sean Liu[1,3], Benhur Lee[3], Florian Krammer[3], Susan Zolla-Pazner[1,3*], Catarina E. Hioe[1,2,3*]

[1]Division of Infectious Diseases, Department of Medicine, Icahn School of Medicine at Mount Sinai, New York, NY USA.

[2]James J. Peters VA Medical Center, Bronx, NY, USA.

[3]Department of Microbiology, Icahn School of Medicine at Mount Sinai, New York, NY, USA.

[4]Graduate School of Biomedical Sciences, Icahn School of Medicine at Mount Sinai, New York, NY, USA.

[5]Department of Pathology, Icahn School of Medicine at Mount Sinai, New York, NY, USA.

[6]Division of Infectious Diseases, Department of Medicine, Mount Sinai West and Morningside, NY, USA.

[7]Pulmonary and Critical Care Medicine, Mount Sinai West, NY, USA.

[8]Global Health Emerging Pathogens Institute, Icahn School of Medicine at Mount Sinai, NY, USA.

[9]Department of Environment Medicine, NYU School of Medicine, New York, NY, USA

*Co-corresponding author

Contact: catarina.hioe@mssm.edu, catarina.hioe@va.gov

Abstract

SARS-CoV-2 has infected millions of people globally. Virus infection requires the receptor-binding domain (RBD) of the spike protein. Although studies have demonstrated anti-spike and -RBD antibodies to be protective in animal models and convalescent plasma as a promising therapeutic option, little is known about immunoglobulin (Ig) isotypes capable of blocking infection. Here, we studied spike- and RBD-specific Ig isotypes in convalescent and acute plasma/sera. We also determined virus neutralization activities in plasma/sera, and purified Ig fractions. Spike- and RBD-specific IgM, IgG1, and IgA1 were produced by all or nearly all subjects at variable levels and detected early after infection. All samples also displayed neutralizing activity. Regression analyses revealed that IgM and IgG1 contributed most to neutralization, consistent with IgM and IgG fractions' neutralization potency. However, IgA also exhibited neutralizing activity at a lower potency. Together, IgG, IgM and IgA are critical components of convalescent plasma used for COVID-19 treatment.

Keywords

SARS-CoV-2, COVID-19, antibody isotypes, neutralization, convalescent plasma

Background

In December 2019, the first patients with coronavirus disease 2019 (COVID-19), caused by severe acute respiratory syndrome coronavirus 2 (SARS-CoV-2), were identified in Wuhan's city of Hubei Province, China[1]. Since then, the epidemic has rapidly spread to most regions of the world, infecting millions of people[2]. Effective therapeutics and vaccines against SARS-CoV-2 are urgently needed. Convalescent plasma transfusion showed promising results in patients with severe to life-threatening COVID-19[3–7] and clinical trials to evaluate the efficacy of convalescent plasma treatment for ambulatory and hospitalized COVID-19 patients are underway[8–11]. To this end, more information about the Ig isotypes present in the plasma of COVID-19 convalescent individuals and their antiviral activities are needed. It is also unclear which of the immunoglobulin (Ig) isotypes present in convalescent plasma are protective. The data would likewise inform vaccine development, as more than 100 vaccine candidates are in different stages of preclinical development, and many are now in phase 2 and 3 clinical trials[12]. Although using different strategies[13], most vaccines are based on the SARS-CoV-2 spike protein[14,15], which is a membrane-anchored protein present with two others (membrane and envelope proteins) on the virus envelope surface and contains the receptor-binding domain (RBD) required for binding to and entry into the cells[16–22]. These vaccines aim to protect by inducing neutralizing antibodies (Abs) capable of blocking viral infection.

Monomeric IgG constitutes approximately 75% of the Abs found in serum and exists as four subtypes: IgG1 (~66% of IgG), IgG2 (~23% of IgG), IgG3 (~7% of IgG) and IgG4 (~4% of IgG)[23,24]. IgM Abs represent 10% of total serum Abs and are the first to arise in response to new antigens[24,25]. Although IgM Abs do not undergo extensive somatic hypermutation to increase their affinity as do IgG and IgA Abs, their higher valency due to oligomerization enhances their

avidity and potency against pathogens[24,26,27]. IgA Abs exist as two subtypes: IgA1 and IgA2, representing 15% of total serum Abs. IgA1 is the primary IgA subtype in serum while IgA2 predominates in mucosal secretions[24]. These two IgA subtypes are dimeric in the mucosa, but in the circulation, they are monomeric.

SARS-CoV-2 spike-, RBD- and nucleocapsid-specific serum/plasma Abs of IgM, IgG, and IgA isotypes are found in most COVID-19 patients[28–35], with Ab neutralizing activities reported developing within the first two weeks of infection and decline over time[31,33,36–38]. However, the neutralizing titers appear to vary greatly[31,33,36–38], and they correlate with Ab binding levels against RBD, spike, and/or nucleocapsid, and with age, duration of symptoms, and symptom severity[31,33,37]. Several RBD-specific monoclonal Abs of IgG isotype with potent antiviral activities have been generated from individuals with high neutralization titers, and these confer protection in animal models[31,36,39,40]. Moreover, a monoclonal Ab of IgA isotype capable of recognizing both the SARS-CoV-1 and SARS-CoV-2 spike proteins and blocking ACE2 receptor binding was recently described[41]. However, no direct evidence is available regarding the neutralizing capacity of plasma IgM and IgA Abs from COVID-19 patients.

Studies on other respiratory viruses such as influenza show that, in addition to IgG, IgA could also mediate virus neutralization, and their relative contribution depends on the physiologic compartment in which they are found, with IgA contributing to the protection of mostly the upper respiratory tract while IgG was protective of the lower respiratory tract[42–45]. Of note, an anti-hemagglutinin monoclonal polymeric IgA has been demonstrated to mediate more potent antiviral activities against influenza when compared to a monoclonal IgG against the same epitope[46]. Interestingly, an IgM Ab with potent antiviral activities targeting influenza B's receptor binding site has also been described[47]. In addition, respiratory syncytial virus (RSV)-

specific mucosal IgA neutralizing Abs are a better correlate of protection than RSV-specific serum IgG neutralizing Abs[48]. In the case of SARS-CoV-1, high titers of mucosal IgA in the lungs correlated with reduced pathology upon viral challenge in animal models[49]. Whether IgA in the blood and in the respiratory tract's mucosa offers protection against SARS-CoV-2 infection or COVID-19 disease remains an open question. Moreover, few data are available regarding the contribution of IgM to neutralization and protection against viruses, including SARS-CoV-2. Of note, in terminally ill COVID-19 patients, systemic SARS-CoV-2 infection affecting multiple organs including the heart, kidneys, and brain, is evident from autopsy studies[50–52]. Thus, the capacity of plasma Ig to suppress virus spread to these organs is critical for effective convalescent plasma therapy against severe COVID-19 disease.

We recently described a multiplex bead Ab binding assay using the Luminex technology to detect total Ig against spike and RBD[53]. Based on this assay, we characterized the Ig isotype profiles against spike and RBD in the plasma and serum from acutely infected or convalescent individuals using this Luminex assay which detects antigen-specific IgM, IgG1-4, IgA1, and IgA2. Using a pseudovirus assay[54], we also measured neutralizing activities in plasma, serum, and Ig isotype plasma fractions to determine the neutralizing capacity of IgM, IgA, and IgG. The data indicated a high prevalence of spike- and RBD-specific IgM and IgA Abs, similar to that of IgG1, in plasma and serum from COVID-19 patients, and their contributions to virus neutralizing activities. By testing purified IgG, IgM and IgA Abs from plasma of convalescent COVID-19 subjects, this study presents the first direct evidence that plasma IgG, IgM, and IgA all contribute to SARS-CoV-2 neutralization.

Results

Levels of Ig isotypes against the SARS-CoV-2 spike and RBD vary in convalescent

individuals. A total of 29 serum (P#5-8) and plasma (TF#1-25) specimens from COVID-19-convalescent individuals was tested. TF#1-25 were collected between March 26 and April 7, 2020, about 4-8 weeks after the initial outbreak in North American, and used for transfusion into hospitalized COVID-19 patients[3]. Ten plasma from COVID-negative contemporaneous blood bank donors (N#4-13) were included for comparison. Sera or plasma from 12 uninfected individuals banked prior to the COVID-19 outbreak (N#1-3 and N#14-22) were used to establish background values. The specimens were initially titrated for total Ig against spike and RBD (**Fig. 1**). All 29 COVID-19 positive specimens exhibited titration curves of total Ig Abs against spike, while none of the negative controls did. Similar results were observed with RBD, except that one contemporaneous COVID-19-negative sample had low levels of RBD-specific Ig (N#10). Overall the background MFI values were higher for RBD than spike. To assess the reproducibility of the assay, the samples were tested in at least two separate experiments run on different days, and a strong correlation was observed between the MFI values from these independent experiments (**Supplementary Fig. 1**). The areas under the curves (AUCs) highly correlated with the MFI values from specimens diluted 1:200 ($p < 0.0001$; **Supplementary Fig. 2**); consequently, all samples were tested for isotyping at this dilution. At the 1:200 dilution we were able to discern a diverse range of Ig isotype levels among individual samples (**Fig. 2**). To evaluate for the presence of spike-specific and RBD-specific total Ig, IgM, IgG1, IgG2, IgG3, IgG4, IgA1 and IgA2, the specificity and strength of the secondary Abs used to detect the different isotypes were first validated with Luminex beads coated with myeloma proteins of known Ig isotypes (IgG1, IgG2, IgG3, IgG4, IgA1, IgA2, and IgM). All eight secondary Abs were able to detect their specific Ig isotypes with MFI values reaching > 60,000 (**Supplementary Fig. 3**).

All 29 convalescent individuals had anti-spike and anti-RBD total Ig (**Fig. 2**), but the Ig levels were highly variable, with MFI values ranging from 36,083 to 190,150. In addition, all 29 convalescent individuals also displayed IgM Abs against spike at varying levels, and 93% were positive for anti-RBD IgM when evaluated using cut-off values calculated as mean + 3 standard deviation (SD) of the 12 pre-pandemic samples (**Fig 2b, c**). An IgG1 response was detected against both spike and RBD in 97% of the convalescent subjects, with MFI values that ranged from 1,013 to 59,880. In contrast, IgG2, IgG3, and IgG4 Abs against spike and RBD were detected in only a small fraction of the subjects, and the levels were very low (MFI values < 1,300) (**Fig. 2**). Surprisingly, almost all individuals produced IgA1 Abs against spike (97%) and RBD (93%), while 17% exhibited IgA2 against spike, and 48% exhibited IgA2 against RBD (**Fig. 2**). Low levels, slightly above cut-off, of spike- and RBD-binding total Ig, IgM, and IgG1, and IgA1 were also detected sporadically in contemporaneous COVID-19 samples, such as N#8, N#10, and N#11. The responses against spike and RBD were highly correlated for every isotype (**Supplementary Fig. 4**). Overall, these data demonstrate that IgM, IgG1, and IgA1 Abs were induced against spike and RBD in all or almost all COVID-19 convalescent individuals (**Fig. 2**). The levels, however, were highly variable among individuals. No statistical significance in the levels of total Ig, IgM, IgG1, and IgA1 was observed between female and male individuals (**Supplementary Fig. 5**).

In **Fig. 3**, regression analyses to assess the impact of individual isotypes on the total Ig binding showed that IgG1 had the highest r^2 values (0.83 and 0.70 for spike- and RBD-binding IgG1, respectively) with $p < 0.0001$, indicating that IgG1 is the major isotype induced by SARS-CoV-2 infection against spike and RBD (**Fig. 3a,b**). IgG2 Abs against RBD had an r^2 value of 0.55 with $p < 0.0001$, but IgG2 levels were very low. For all other isotypes, including IgM, the r^2

values were less than 0.40 (**Fig. 3c**). Thus, despite the presence of many isotypes in sera and plasma, as expected, the major isotype is IgG1.

Specimens from two patients (P#1 and P#2) were drawn during the acute phase of the infection. Serial specimens from these patients were tested to determine the isotypes of Abs present early in infection. The earliest samples from both patients, drawn at 7 or 8 days after symptom onset were already positive for total Ig, IgG1, IgA1and IgM Abs against spike (**Supplementary Fig. 6a**) and RBD (**Supplementary Fig. 6b**), and these levels increased over the following three to seven days. On the contrary, IgA2 Ab levels were near or below background on days 7-8 and remained unchanged over two weeks post-onset. IgG4 Abs also remained low or near background, whereas IgG2 and IgG3 Abs increased slightly to above background after 10-15 days.

Neutralizing activities are detected in all convalescent COVID-19 individuals. We subsequently tested the ability of samples from convalescent subjects to neutralize a VSVΔG pseudovirus bearing the SARS-CoV-2 spike protein (COV2pp). This pseudovirus assay demonstrated a strong positive correlation with neutralization of the authentic SARS-CoV-2 virus ($p = 0.82$ and $p < 0.0001$ for IC_{50} correlation)[54]. The results, shown in **Fig. 4**, demonstrate the percentages of COV2pp neutralizing activity in serum or plasma specimens from 28 COVID-19-convalescent individuals and 11 COVID-19-negative individuals over a range of seven serial four-fold dilutions. A soluble recombinant RBD (sRBD) protein capable of blocking virus infection was tested in parallel as a positive control.

All specimens from COVID-19-convalescent individuals were able to neutralize the virus at levels above 50% (**Fig. 4a**). For 26 of 28 specimens, neutralization reached more than 90% (**Fig. 4a**). The sample with the lowest titer (reciprocal IC_{50} titer = 37) reached a neutralization

plateau of only ~60%. Of note, one sample (TF#11) demonstrated highly potent neutralization with a reciprocal IC_{50} titer > 40,960, and neutralization was still 75% at the highest dilution tested. None of the samples from COVID-19-negative individuals reached 50% neutralization (**Fig. 4b**), while the sRBD positive control demonstrated potent neutralization with an IC_{50} of 0.06 µg/mL (**Fig. 4c**), similar to that recently reported[54].

The samples were also tested for neutralization against a COV2pp bearing spike with a D614 mutation (D614G mutant), as the D614G variant has become the most prevalent circulating strain in the global pandemic[55]. Similar to the WT COV2pp, all COVID-19-convalescent samples had neutralizing activity reaching >50% (**Fig. 4d**), while none of the negative samples did (**Fig. 4e**). The IC_{90} titers against WT and D614 mutant differed on average by only 1.7-fold and correlated strongly with each other (**Fig. 4f**).

IgM and IgG1 contribute most to SARS-CoV-2 neutralization. Given our observation that Ab isotype levels and neutralization titers varied tremendously among convalescent COVID-19 individuals (**Figs. 2 and 5**), we investigated the relative contribution of each Ab isotype to the neutralizing activities. Regression analyses were performed on 27 COVID-19-convalescent samples (TF#11 was excluded due to its outlier neutralization titer). As expected, relatively high r^2 values (0.32 – 0.62) and significant p values were observed with total Ig, IgM and IgG1; in each case, r^2 values were higher for spike than for RBD (**Fig. 6a**). For other isotypes, significant p values were sporadically achieved, but r^2 values were weak (**Fig. 6a,b**).

Neutralizing activities are mediated by IgM, IgG, and IgA fractions. To assess directly the capacity of different isotypes to mediate neutralization, we evaluated the neutralization activities of IgM, IgG, and IgA fractions purified from the plasma of five COVID-19-convalescent individuals (RP#1-5). The enrichment of IgM, IgG1, and IgA1 Abs reactive

with spike and RBD was validated using the isotyping method used above (**Supplementary Fig. 7** and not shown). These IgM, IgG, and IgA fractions were then evaluated for neutralizing activity along with the original plasma (**Fig. 7**). The RP#1-5 plasma neutralizing reciprocal IC_{50} titers ranged from 35 to 690 (**Fig. 7a,b**). Purified IgM and IgG fractions from RP#1-5 all mediated neutralization reaching more than 50%. Unexpectedly, plasma IgA fractions also displayed neutralizing activity, although not to the same potency as IgM and IgG (**Fig 7c,d**). In contrast, IgM, IgG, and IgA fractions from the negative control (RN#1) showed no neutralization (**Fig. 7c,d**).

Discussion

Our study demonstrated that IgG1, IgA1 and IgM Abs against spike and RBD were highly prevalent in the plasma samples of convalescent COVID-19 patients approximately one to two months after infection. The presence of these isotypes was detected within 7-8 days after the onset of symptoms. Importantly, all three isotypes show the capacity to mediate virus neutralization. While regression analyses indicate the strongest contribution of IgM and IgG1 Abs to neutralizing activity, direct testing of purified isotype fractions showed that IgA also contributed to neutralizing activity, indicating the protective potential of all three major Ig isotypes. These data carry important implications for the use of convalescent plasma and hyperimmunoglobulin as COVID-19 therapeutic modalities, suggesting that the selection be based on the measurement of all of these Ig isotypes.

While all COVID-19 convalescent individuals exhibited plasma/serum neutralization activities reaching 50% neutralization, and 26 of 28 specimens attained 90% neutralization, neutralization levels were highly variable with reciprocal IC_{50} and IC_{90} titers ranging over three orders of magnitude. The titers were comparable against the initial Wuhan strain and the

currently prevalent D614G strain. Similarly, the levels of spike- and RBD-binding total Ig and Ig isotypes varied greatly.

A trend toward higher levels of total Ig and each Ig isotype was seen in female compared to male subjects, as reported in another study[56]. Moreover, except for TF#11 (a male elite neutralizer), the median neutralizing reciprocal IC_{90} titer was higher in females than males, although the difference did not reach significance (data not shown). Sex differences in Ab induction have been observed following vaccination against influenza in humans and mice and were shown to result from the impact of sex steroids[57,58]. Whether and to what extent this contributes to sex differences seen in clinical outcomes of COVID-19[59] remains to be investigated. Other studies have shown that the Ab levels were associated with multiple factors, including time from disease onset[60] and disease severity[30]. However, other than sex, clinical data are not available for the subjects studied here, limiting our analysis only to neutralization and Ig isotypes.

One remarkable finding from our study is that although neutralization titers correlated with binding levels of IgM and IgG1 and not with those of IgA1 or IgA2, purified IgA fractions from convalescent COVID-19 patients exhibited significant neutralizing activities. The importance of this finding is underscored by the data showing that IgA1 was the prominent isotype in some plasma samples such as TF#7 and TF#24 and that IgA1 could be detected early, within a week after symptom onset. Data from other studies also supported IgA's significance in that purified IgA fractions exhibited more or as potent neutralizing activities compared to purified IgG and that RBD-binding IgA correlated as strongly as the IgG equivalent with micro-neutralization titers[61,62]. The presence of IgA was also detected in the saliva and bronchoalveolar lavage samples from COVID-19 patients[62,63]. Nonetheless, Wang *et al.* reported that plasma IgA

monomers were less potent than the plasma IgG and secretory IgA counterparts[64]. In our study, neutralization activities detected in the IgA fractions were mediated mainly by IgA1, the predominant IgA isotype in the plasma, and the IC_{50} potency of the IgA fraction was ~4-fold lower than those of IgM and IgG1 fractions. This difference cannot be explained entirely by lower amounts of spike-specific IgA1 in the tested fractions, as estimations using spike-specific monoclonal antibodies of the respective isotypes yielded similar concentrations in IgA1 and IgM fractions (median of 2 and 2.5 µg/mL respectively). Fine epitope specificity and affinity may differ for IgA, IgM, and IgG to impact neutralization potency, but are yet to be evaluated.

In addition to neutralization, non-neutralizing Ab activities have been implicated in protection from virus infection through potent Fc-mediated functions such as antibody-dependent cellular cytotoxicity (ADCC), antibody-dependent cellular phagocytosis (ADCP), and complement-mediated lysis; this is reported for HIV, influenza, Marburg, and Ebola viruses[44,65–68]. The Fc activities were not evaluated in our study, and their contribution to protection against infection and disease progression in humans is yet unclear[15,69–71]. Interestingly, a recent study demonstrated enrichment of spike-specific IgM and IgA1 Abs and spike-specific phagocytic and antibody-dependent complement deposition (ADCD) activity in plasma of individuals who recovered from a SARS-CoV-2 infection, while nucleocapsid-specific IgM and IgA2 responses and nucleocapsid-specific ADCD activity were features enriched in deceased patients[72]. DNA vaccines expressing full-length and truncated spike proteins could curtail SARS-CoV-2 infection in the respiratory tract by varying degrees in rhesus macaques. Virus reduction correlated with levels of neutralization and also Fc-mediated effector functions such as ADCD[15]. Interestingly, these DNA vaccines elicited spike- and RBD-specific IgG1, IgG2, IgG3, IgA, and IgM Abs, and similar to our findings, neutralization correlated most strongly with IgM. Adenovirus serotype 26

vaccine vectors encoding seven different SARS-CoV-2 spike variants showed varying protection levels, and virus reduction correlated best with neutralizing Ab titers together with IgM binding levels, FcγRII-binding, and ADCD responses[73]. Defining the full potential of Abs against SARS-CoV-2 that includes neutralizing, non-neutralizing and enhancing activities are vital for determining the optimal convalescent Ab treatment against COVID-19 and assessing the potential efficacy of COVID-19 vaccine candidates.

When we examined plasma specimens collected within 7-8 days after COVID-19 symptom onset, we detected IgG and IgA against spike and RBD, as well as IgM. This is consistent with published reports showing that 100% of COVID-19-infected individuals developed IgG within 19 days after symptom onset and that seroconversion for IgG and IgM occurred simultaneously or sequentially[30]. IgA was also found early after infection (4-6 days after symptom onset) and increased over time in several other studies[28,35,63,74]. These studies suggest that measuring total Ig, rather than IgG, would provide a better outcome for early disease diagnosis. Indeed, we found no correlation between the levels of different isotypes examined in our study (data not shown). This lack of correlation may result from their asynchronous, sequential induction (IgM first, then IgG, and finally IgA). Still, IgA's presence early during acute infection also suggests the potential contribution of natural IgA, which, similar to natural IgM, arises spontaneously from innate B1 cells to provide the initial humoral responses before the induction, maturation, and class-switching of adaptive classical B cells[75,76].

In summary, this study demonstrates that spike- and RBD-specific IgM, IgG1, and IgA1 Abs were present in serum and plasma of all or almost all analyzed COVID-19 convalescent subjects and were detected at very early stages of infection. The plasma of convalescent individuals also displayed neutralization activities mediated by IgM, IgG, and IgA1, although

297 neutralization titers correlated more strongly with IgM and IgG levels. The contribution of IgM,
298 IgG, and IgA Abs to the neutralizing activities against SARS-CoV-2 demonstrates their
299 importance in the efficacy of convalescent plasma used for COVID-19 treatment.

300 ## Methods

301 **Recombinant proteins.** The recombinant spike and RBD proteins were produced as
302 previously described[77] in Expi293F cells (ThermoFisher) by transfections of purified DNA using
303 an ExpiFectamine Transfection Kit (ThermoFisher). The soluble version of the spike protein
304 included the protein ectodomain (amino acids 1-1213), a C-terminal thrombin cleavage site, a T4
305 foldon trimerization domain, and a hexahistidine tag. The protein sequence was also modified to
306 remove the polybasic cleavage site (RRAR to A) and two stabilizing mutations (K986P and
307 V987P, wild type numbering). The RBD (amino acids 319-541) included the signal peptide
308 (amino acids 1–14) and a hexahistidine tag. Supernatants from transfected cells were harvested
309 three days after the transfection by centrifugation of the culture at 4000 g for 20 minutes. The
310 supernatant was then incubated with 6 mL Ni-NTA agarose (Qiagen) for one to two hours at
311 room temperature. Next, gravity-flow columns were used to collect the Ni-NTA agarose, and the
312 protein was eluted. Each protein was concentrated in Amicon centrifugal units (EMD Millipore)
313 and resuspended in phosphate buffered saline (PBS).

314 **Human samples.** Twenty-five citrated plasma of convalescent COVID-19 individuals
315 destined for transfusion to SARS-CoV-2-infected individuals (TF#1-25, collected between
316 March 26th and April 7th 2020) and ten specimens derived from the blood bank (N#4-13),
317 representing contemporary COVID-19-negative blood bank donors, were obtained from the
318 Division of Transfusion Medicine of the Department of Pathology, Molecular and Cell-Based
319 Medicine (Mount Sinai Hospital System, IRB #20-03574). Four additional de-identified serum

specimens from individuals with COVID-19 (P#5-8) were provided by the Clinical Pathology Division of the Department of Pathology, Molecular and Cell-Based Medicine at the Icahn School of Medicine at Mount Sinai. Serum and plasma samples were also obtained from study participants enrolled in IRB-approved protocols at the Icahn School of Medicine at Mount Sinai (Icahn School of Medicine at Mount Sinai IRB #16-00772, #16-00791, #17-01243) and the James J. Peter VA Medical Center (IRB #BAN-1604). Samples from these protocols included sera from seven participants with documented SARS-CoV-2 infection (P#1 d8, d11, and d15 after symptom onset, P#2 d7 and d10 after symptom onset, and RP#1-5 after convalescence), and sera from twelve healthy donors (N#1-3, N#14-22) collected prior to the spread of SARS-CoV-2 in the USA. All study participants provided written consent at enrollment and agreed to sample banking and future research use of their banked biospecimens. All samples were heat-inactivated and/or treated with 0.05% Triton X-100 prior to use.

Ig fractionation. IgA was first isolated from plasma by mixing 1:2 diluted plasma with peptide M agarose beads (600 µL/28 mL plasma, InvivoGen #GEL-PDM) for 1.5 hours at room temperature. Beads were then collected on a column and washed with PBS until protein reading (280 nm) by Nanodrop reached background. IgA was eluted from beads with a pH 2.8 elution buffer (Thermo Scientific #21004) and neutralized with pH 9 Tris buffer. The pass-through plasma sample was collected for IgG enrichment using protein G agarose beads (InvivoGen #GEL-AGG) using the same protocol as above and subsequently for IgM isolation using a HiTrap IgM column (G.E. Healthcare #17-5110-01) according to the manufacturer's instruction. An additional purification step was performed using Protein A Plus mini-spin columns to separate IgG from IgM. Protein concentrations were determined with Nanodrop prior to use in Luminex and neutralization experiments.

Multiplex bead Ab binding assay. The SARS-CoV-2 antigens used in this assay consisted of a soluble recombinant trimerized form of the spike protein and a recombinant RBD protein[78]. Antigens were coupled to beads as previously described, with minor changes[53]. Each antigen was covalently coupled individually to a uniquely labeled fluorochrome carboxylated xMAP bead set at 2.0 μg protein/million beads using a two-step carbodiimide reaction with the xMAP Ab Coupling (AbC) Kit following to the manufacturers' instructions (Luminex, Austin, TX). The coupled beads were pelleted, resuspended at $5x10^6$ beads/mL in storage buffer (PBS, 0.1% bovine serum albumin (BSA), 0.02% Tween-20, and 0.05% sodium azide, pH 7.4), and stored at -80˚C. Three to five million beads per batch were prepared in a 1.5 mL conical tube.

Before each experiment, the beads needed for a single run (2,500 beads/well x number of wells) were pelleted and resuspended in assay buffer (PBS, 0.1% B.S.A., 0.02% Tween-20) to deliver 2,500 beads in a volume of 50 μL/well in a 96-well plate. Sera/plasma samples were serially titrated (1:50 to 1:6400 final dilution) or diluted in assay buffer to 1:100 (for a final dilution of 1:200). The samples were then added as 50 μL/well to the wells containing the beads and incubated at room temperature for 1 hour at 600 rpm. After two washes in assay buffer, 100 μL/well of biotinylated antibodies specific for total Ig, IgG1, IgG2, IgG3, IgG4, IgA1, IgA2, or IgM was added and incubated for 30 minutes at room temperature on a plate shaker; these antibodies were rabbit biotinylated-anti-human total Ig (Abcam, catalog #ab97158) at 2 μg/mL, mouse biotinylated-anti-human IgG1 Fc (Invitrogen #MH1515) at 4 μg/mL, mouse biotinylated-anti-human IgG2 Fc (Southern Biotech #9060-08) at 1 μg/mL, mouse biotinylated-anti-human IgG3 Hinge (Southern Biotech #9210-08) at 3 μg/mL, mouse biotinylated-anti-human IgG4 Fc (Southern Biotech #9200-08) at 4 μg/mL, mouse biotinylated-anti-human IgA1 Fc (Southern Biotech #9130-08) at 4 μg/mL, mouse biotinylated-anti-human IgA2 Fc (Southern Biotech

#9140-08) at 4 µg/mL or goat biotinylated-anti-human IgM (Southern Biotech #2020-08) at 3 µg/mL. After two washes, 100 µL/well of Streptavidin-Phycoerythrin (P.E.) at 1 µg/mL was added (BioLegend #405204) followed by a 30 minutes incubation at room temperature on a plate shaker. After two additional washes, 100 µL of assay buffer/well was added and put on a shaker to resuspend the beads. Each plate was read with a Luminex Flexmap 3D instrument. Specimens were tested in duplicate, and the results were recorded as mean fluorescent intensity (MFI).

COV2pp production and titration. The SARS-CoV-2 pseudoviruses (COV2pp) with wild-type (WT) or D614G mutated spike proteins were produced as previously described[54]. Briefly, 293T cells were transfected to overexpress SARS-CoV-2 glycoproteins. For background entry with particles lacking a viral surface glycoprotein, pCAGG empty vector was transfected into 293T cells. Around 8 hours post-transfection, cells were infected with the VSVΔG-rLuc reporter virus for 2 hours and then washed with PBS. Two days post-infection, supernatants were collected and clarified by centrifugation at 1250 rpm for 5 minutes. At the time of collection, a small batch of VSVΔG-rLuc particles bearing the CoV2pp was treated with TPCK-treated trypsin (Sigma-Aldrich #T1426-1G) at room temperature for 15 minutes prior to inhibition with soybean trypsin inhibitor (Fisher Scientific #1707502). Finally, particles were aliquoted prior to storage in -80˚C.

The pseudoviruses were titrated on 20,000 Vero-CCL81 cells seeded in a 96-well black plate with clear bottom 24 hours before infection. At 18 to 22 hours post-infection, the infected cells were washed with PBS and processed for detection of Renilla luciferase activity with Renilla-Glo™ Luciferase Assay System (Promega #E2720). A Cytation3 (BioTek) instrument was used to read luminescence.

COV2pp neutralization. The day before infection, 20,000 Vero-CCL81 cells per well

were seeded in a 96-well black plate with clear bottom. On the assay day, the COV2pp WT or D614G virus was diluted based on the titration results, and 82.5 µL added to all wells, except six for cell control, of a 96-well V-bottom plate. The seven serial dilutions of the samples were then prepared in another 96-well V-bottom plate. Samples of the COVID-19-infected individuals and COVID-19-negative individuals were tested at 4-fold dilutions from 1:10 to 1:40,960. Purified IgM, IgG, and IgA fractions and negative control fractions were tested at 4-fold dilutions from 500 to 0.02 µg/mL. 27.5 µL per well of the diluted sample was then added to the plate with the pseudovirus. For each plate, six wells were kept with the virus only, as virus control, and six wells with media only, as cell control. The plates were then incubated for 30 minutes at room temperature. 100 µL of the virus/sample mix or virus or medium alone was then added to the cells and spinoculated by centrifugation at 1250 rpm for 1 hour at room temperature. After incubation for 18 to 22 hours at 37˚C, the measurement of infection/neutralization was performed as described for the COV2pp titration.

The percentage of neutralization was calculated with the formula: 100-((sample's R.L.U. – cell control R.L.U.) / virus control R.L.U.) *100). The inhibitory concentration 50% (IC_{50}) and 90% (IC_{90}) were respectively defined as the reciprocal sample dilution or purified Ig fraction concentration achieving 50% and 90% neutralization.

Statistical analysis. Statistical tests that included two-tailed Mann-Whitney test, Spearman rank-order correlation test, and simple linear regressions were performed as designated in the figure legends. All statistical tests were performed using GraphPad Prism 8.

Data availability.

411 The raw data that support the findings of this study are available from the corresponding
412 author upon request.
413
414
415 **References.**
416 1. Zhu N, Zhang D, Wang W, Li X, Yang B, Song J, et al. A Novel Coronavirus from
417 Patients with Pneumonia in China, 2019. N Engl J Med. 2020 20;382(8):727–33.
418 2. WHO Coronavirus Disease (COVID-19) Dashboard [Internet]. [cited 2020 Jun 29].
419 Available from: https://covid19.who.int
420 3. Liu STH, Lin H-M, Baine I, Wajnberg A, Gumprecht JP, Rahman F, et al. Convalescent
421 plasma treatment of severe COVID-19: a propensity score-matched control study. Nat Med.
422 2020 Sep 15;
423 4. Martinez-Resendez MF, Castilleja-Leal F, Torres-Quintanilla A, Rojas-Martinez A,
424 Garcia-Rivas G, Ortiz-Lopez R, et al. Initial experience in Mexico with convalescent plasma in
425 COVID-19 patients with severe respiratory failure, a retrospective case series. medRxiv. 2020
426 Jul 20;2020.07.14.20144469.
427 5. Altuntas F, Ata N, Yigenoglu TN, Bascı S, Dal MS, Korkmaz S, et al. Convalescent
428 plasma therapy in patients with COVID-19. Transfus Apher Sci Off J World Apher Assoc Off J
429 Eur Soc Haemapheresis. 2020 Sep 19;102955.
430 6. Zeng H, Wang D, Nie J, Liang H, Gu J, Zhao A, et al. The efficacy assessment of
431 convalescent plasma therapy for COVID-19 patients: a multi-center case series. Signal Transduct
432 Target Ther. 2020 Oct 6;5(1):1–12.
433 7. Ibrahim D, Dulipsingh L, Zapatka L, Eadie R, Crowell R, Williams K, et al. Factors

Associated with Good Patient Outcomes Following Convalescent Plasma in COVID-19: A Prospective Phase II Clinical Trial. Infect Dis Ther. 2020 Sep 20;1–14.

8. Janssen M, Schäkel U, Fokou CD, Krisam J, Stermann J, Kriegsmann K, et al. A Randomized Open label Phase-II Clinical Trial with or without Infusion of Plasma from Subjects after Convalescence of SARS-CoV-2 Infection in High-Risk Patients with Confirmed Severe SARS-CoV-2 Disease (RECOVER): A structured summary of a study protocol for a randomised controlled trial. Trials. 2020 Dec;21(1):1–4.

9. NIH expands clinical trials to test convalescent plasma against COVID-19 [Internet]. National Institutes of Health (NIH). 2020 [cited 2020 Oct 7]. Available from: https://www.nih.gov/news-events/news-releases/nih-expands-clinical-trials-test-convalescent-plasma-against-covid-19

10. Convalescent Plasma to Limit SARS-CoV-2 Associated Complications - Full Text View - ClinicalTrials.gov [Internet]. [cited 2020 Nov 2]. Available from: https://clinicaltrials.gov/ct2/show/NCT04373460

11. Convalescent Plasma in Outpatients With COVID-19 - Full Text View - ClinicalTrials.gov [Internet]. [cited 2020 Nov 2]. Available from: https://clinicaltrials.gov/ct2/show/NCT04355767

12. Le TT, Andreadakis Z, Kumar A, Román RG, Tollefsen S, Saville M, et al. The COVID-19 vaccine development landscape. Nat Rev Drug Discov. 2020 Apr 9;19(5):305–6.

13. Amanat F, Krammer F. SARS-CoV-2 Vaccines: Status Report. Immunity. 2020 Apr 3;

14. Mulligan MJ, Lyke KE, Kitchin N, Absalon J, Gurtman A, Lockhart SP, et al. Phase 1/2 Study to Describe the Safety and Immunogenicity of a COVID-19 RNA Vaccine Candidate (BNT162b1) in Adults 18 to 55 Years of Age: Interim Report. medRxiv. 2020 Jul

1;2020.06.30.20142570.

15. Yu J, Tostanoski LH, Peter L, Mercado NB, McMahan K, Mahrokhian SH, et al. DNA vaccine protection against SARS-CoV-2 in rhesus macaques. Science. 2020 May 20;

16. Yan R, Zhang Y, Li Y, Xia L, Guo Y, Zhou Q. Structural basis for the recognition of SARS-CoV-2 by full-length human ACE2. Science. 2020 27;367(6485):1444–8.

17. Hoffmann M, Kleine-Weber H, Krüger N, Müller M, Drosten C, Pöhlmann S. The novel coronavirus 2019 (2019-nCoV) uses the SARS-coronavirus receptor ACE2 and the cellular protease TMPRSS2 for entry into target cells. bioRxiv. 2020 Jan 31;2020.01.31.929042.

18. Wang K, Chen W, Zhou Y-S, Lian J-Q, Zhang Z, Du P, et al. SARS-CoV-2 invades host cells via a novel route: CD147-spike protein. bioRxiv. 2020 Mar 14;2020.03.14.988345.

19. Zhou P, Yang X-L, Wang X-G, Hu B, Zhang L, Zhang W, et al. A pneumonia outbreak associated with a new coronavirus of probable bat origin. Nature. 2020;579(7798):270–3.

20. Lu R, Zhao X, Li J, Niu P, Yang B, Wu H, et al. Genomic characterisation and epidemiology of 2019 novel coronavirus: implications for virus origins and receptor binding. Lancet Lond Engl. 2020 22;395(10224):565–74.

21. Hoffmann M, Kleine-Weber H, Schroeder S, Krüger N, Herrler T, Erichsen S, et al. SARS-CoV-2 Cell Entry Depends on ACE2 and TMPRSS2 and Is Blocked by a Clinically Proven Protease Inhibitor. Cell. 2020 16;181(2):271-280.e8.

22. Walls AC, Park Y-J, Tortorici MA, Wall A, McGuire AT, Veesler D. Structure, Function, and Antigenicity of the SARS-CoV-2 Spike Glycoprotein. Cell. 2020 16;181(2):281-292.e6.

23. Vidarsson G, Dekkers G, Rispens T. IgG Subclasses and Allotypes: From Structure to Effector Functions. Front Immunol [Internet]. 2014 Oct 20 [cited 2018 Jun 12];5. Available

480 from: https://www.ncbi.nlm.nih.gov/pmc/articles/PMC4202688/

481 24. Schroeder HW, Cavacini L. Structure and function of immunoglobulins. J Allergy Clin

482 Immunol. 2010 Feb;125(2 Suppl 2):S41-52.

483 25. Boes M. Role of natural and immune IgM antibodies in immune responses. Mol

484 Immunol. 2000 Dec;37(18):1141–9.

485 26. Müller R, Gräwert MA, Kern T, Madl T, Peschek J, Sattler M, et al. High-resolution

486 structures of the IgM Fc domains reveal principles of its hexamer formation. Proc Natl Acad Sci.

487 2013 Jun 18;110(25):10183–8.

488 27. Brekke OH, Sandlie I. Therapeutic antibodies for human diseases at the dawn of the

489 twenty-first century. Nat Rev Drug Discov. 2003 Jan;2(1):52–62.

490 28. Ma H, Zeng W, He H, Zhao D, Jiang D, Zhou P, et al. Serum IgA, IgM, and IgG

491 responses in COVID-19. Cell Mol Immunol. 2020 Jul;17(7):773–5.

492 29. Grifoni A, Weiskopf D, Ramirez SI, Mateus J, Dan JM, Moderbacher CR, et al. Targets

493 of T Cell Responses to SARS-CoV-2 Coronavirus in Humans with COVID-19 Disease and

494 Unexposed Individuals. Cell. 2020 Jun 25;181(7):1489-1501.e15.

495 30. Long Q-X, Liu B-Z, Deng H-J, Wu G-C, Deng K, Chen Y-K, et al. Antibody responses

496 to SARS-CoV-2 in patients with COVID-19. Nat Med. 2020 Jun;26(6):845–8.

497 31. Robbiani DF, Gaebler C, Muecksch F, Lorenzi JCC, Wang Z, Cho A, et al. Convergent

498 antibody responses to SARS-CoV-2 in convalescent individuals. Nature. 2020 Jun 18;

499 32. Zhao J, Yuan Q, Wang H, Liu W, Liao X, Su Y, et al. Antibody responses to SARS-

500 CoV-2 in patients of novel coronavirus disease 2019. Clin Infect Dis Off Publ Infect Dis Soc

501 Am. 2020 Mar 28;

502 33. Okba NMA, Müller MA, Li W, Wang C, GeurtsvanKessel CH, Corman VM, et al.

503 Severe Acute Respiratory Syndrome Coronavirus 2-Specific Antibody Responses in Coronavirus
504 Disease Patients. Emerg Infect Dis. 2020 Jul;26(7):1478–88.
505 34. Guo L, Ren L, Yang S, Xiao M, Chang D, Yang F, et al. Profiling Early Humoral
506 Response to Diagnose Novel Coronavirus Disease (COVID-19). Clin Infect Dis Off Publ Infect
507 Dis Soc Am. 2020 Mar 21;
508 35. Padoan A, Sciacovelli L, Basso D, Negrini D, Zuin S, Cosma C, et al. IgA-Ab response
509 to spike glycoprotein of SARS-CoV-2 in patients with COVID-19: A longitudinal study. Clin
510 Chim Acta. 2020 Aug 1;507:164–6.
511 36. Ju B, Zhang Q, Ge J, Wang R, Sun J, Ge X, et al. Human neutralizing antibodies elicited
512 by SARS-CoV-2 infection. Nature. 2020 May 26;
513 37. Wu F, Wang A, Liu M, Wang Q, Chen J, Xia S, et al. Neutralizing antibody responses to
514 SARS-CoV-2 in a COVID-19 recovered patient cohort and their implications. medRxiv. 2020
515 Apr 20;2020.03.30.20047365.
516 38. Prévost J, Gasser R, Beaudoin-Bussières G, Richard J, Duerr R, Laumaea A, et al. Cross-
517 Sectional Evaluation of Humoral Responses against SARS-CoV-2 Spike. Cell Rep Med. 2020
518 Oct 20;1(7):100126.
519 39. Rogers TF, Zhao F, Huang D, Beutler N, Burns A, He W, et al. Isolation of potent SARS-
520 CoV-2 neutralizing antibodies and protection from disease in a small animal model. Science
521 [Internet]. 2020 Jun 15 [cited 2020 Jul 16]; Available from:
522 https://science.sciencemag.org/content/early/2020/06/15/science.abc7520
523 40. Zost SJ, Gilchuk P, Case JB, Binshtein E, Chen RE, Nkolola JP, et al. Potently
524 neutralizing and protective human antibodies against SARS-CoV-2. Nature. 2020 Jul 15;1–10.
525 41. Ejemel M, Li Q, Hou S, Schiller ZA, Wallace AL, Amcheslavsky A, et al. IgA MAb

526 blocks SARS-CoV-2 Spike-ACE2 interaction providing mucosal immunity. BioRxiv Prepr Serv
527 Biol. 2020 May 15;
528 42. Renegar KB, Small PA, Boykins LG, Wright PF. Role of IgA versus IgG in the control of
529 influenza viral infection in the murine respiratory tract. J Immunol Baltim Md 1950. 2004 Aug
530 1;173(3):1978–86.
531 43. Suzuki T, Kawaguchi A, Ainai A, Tamura S, Ito R, Multihartina P, et al. Relationship of
532 the quaternary structure of human secretory IgA to neutralization of influenza virus. Proc Natl
533 Acad Sci U S A. 2015 Jun 23;112(25):7809–14.
534 44. Krammer F. The human antibody response to influenza A virus infection and vaccination.
535 Nat Rev Immunol. 2019;19(6):383–97.
536 45. Reynolds HY. Immunoglobulin G and its function in the human respiratory tract. Mayo
537 Clin Proc. 1988 Feb;63(2):161–74.
538 46. Muramatsu M, Yoshida R, Yokoyama A, Miyamoto H, Kajihara M, Maruyama J, et al.
539 Comparison of antiviral activity between IgA and IgG specific to influenza virus hemagglutinin:
540 increased potential of IgA for heterosubtypic immunity. PloS One. 2014;9(1):e85582.
541 47. Shen C, Zhang M, Chen Y, Zhang L, Wang G, Chen J, et al. An IgM antibody targeting
542 the receptor binding site of influenza B blocks viral infection with great breadth and potency.
543 Theranostics. 2019;9(1):210–31.
544 48. Habibi MS, Jozwik A, Makris S, Dunning J, Paras A, DeVincenzo JP, et al. Impaired
545 Antibody-mediated Protection and Defective IgA B-Cell Memory in Experimental Infection of
546 Adults with Respiratory Syncytial Virus. Am J Respir Crit Care Med. 2015 May 1;191(9):1040–
547 9.
548 49. Du L, He Y, Zhou Y, Liu S, Zheng B-J, Jiang S. The spike protein of SARS-CoV--a

549 target for vaccine and therapeutic development. Nat Rev Microbiol. 2009 Mar;7(3):226–36.

550 50. Schurink B, Roos E, Radonic T, Barbe E, Bouman CSC, de Boer HH, et al. Viral

551 presence and immunopathology in patients with lethal COVID-19: a prospective autopsy cohort

552 study. Lancet Microbe. 2020 Sep 25;

553 51. Lindner D, Fitzek A, Bräuninger H, Aleshcheva G, Edler C, Meissner K, et al.

554 Association of Cardiac Infection With SARS-CoV-2 in Confirmed COVID-19 Autopsy Cases.

555 JAMA Cardiol. 2020 Jul 27;

556 52. Remmelink M, De Mendonça R, D'Haene N, De Clercq S, Verocq C, Lebrun L, et al.

557 Unspecific post-mortem findings despite multiorgan viral spread in COVID-19 patients. Crit

558 Care Lond Engl. 2020 12;24(1):495.

559 53. Weiss S, Klingler J, Hioe C, Amanat F, Baine I, Kojic EM, et al. A High Through-put

560 Assay for Circulating Antibodies Directed against the S Protein of Severe Acute Respiratory

561 Syndrome Corona virus 2. medRxiv. 2020 Apr 17;2020.04.14.20059501.

562 54. Oguntuyo KY, Stevens CS, Hung C-T, Ikegame S, Acklin JA, Kowdle SS, et al.

563 Quantifying absolute neutralization titers against SARS-CoV-2 by a standardized virus

564 neutralization assay allows for cross-cohort comparisons of COVID-19 sera. medRxiv. 2020

565 Aug 15;2020.08.13.20157222.

566 55. Korber B, Fischer WM, Gnanakaran S, Yoon H, Theiler J, Abfalterer W, et al. Tracking

567 Changes in SARS-CoV-2 Spike: Evidence that D614G Increases Infectivity of the COVID-19

568 Virus. Cell. 2020 Aug 20;182(4):812-827.e19.

569 56. Zeng F, Dai C, Cai P, Wang J, Xu L, Li J, et al. A comparison study of SARS-CoV-2 IgG

570 antibody between male and female COVID-19 patients: a possible reason underlying different

571 outcome between gender. medRxiv. 2020 Mar 27;2020.03.26.20040709.

572 57. Fink AL, Engle K, Ursin RL, Tang W-Y, Klein SL. Biological sex affects vaccine
573 efficacy and protection against influenza in mice. Proc Natl Acad Sci U S A. 2018
574 04;115(49):12477–82.
575 58. Potluri T, Fink AL, Sylvia KE, Dhakal S, Vermillion MS, vom Steeg L, et al. Age-
576 associated changes in the impact of sex steroids on influenza vaccine responses in males and
577 females. Npj Vaccines. 2019 Jul 12;4(1):1–12.
578 59. Jin J-M, Bai P, He W, Wu F, Liu X-F, Han D-M, et al. Gender Differences in Patients
579 With COVID-19: Focus on Severity and Mortality. Front Public Health [Internet]. 2020 [cited
580 2020 Aug 6];8. Available from:
581 https://www.frontiersin.org/articles/10.3389/fpubh.2020.00152/full
582 60. Long Q-X, Tang X-J, Shi Q-L, Li Q, Deng H-J, Yuan J, et al. Clinical and
583 immunological assessment of asymptomatic SARS-CoV-2 infections. Nat Med. 2020 Jun 18;1–
584 5.
585 61. Mazzini L, Martinuzzi D, Hyseni I, Lapini G, Benincasa L, Piu P, et al. Comparative
586 analyses of SARS-CoV-2 binding (IgG, IgM, IgA) and neutralizing antibodies from human
587 serum samples. bioRxiv. 2020 Aug 10;2020.08.10.243717.
588 62. Sterlin D, Mathian A, Miyara M, Mohr A, Anna F, Claer L, et al. IgA dominates the early
589 neutralizing antibody response to SARS-CoV-2. medRxiv. 2020 Jun 11;2020.06.10.20126532.
590 63. Isho B, Abe KT, Zuo M, Jamal AJ, Rathod B, Wang JH, et al. Persistence of serum and
591 saliva antibody responses to SARS-CoV-2 spike antigens in COVID-19 patients. Sci Immunol
592 [Internet]. 2020 Oct 8 [cited 2020 Oct 9];5(52). Available from:
593 https://immunology.sciencemag.org/content/5/52/eabe5511
594 64. Wang Z, Lorenzi JCC, Muecksch F, Finkin S, Viant C, Gaebler C, et al. Enhanced

595 SARS-CoV-2 Neutralization by Secretory IgA in vitro. bioRxiv. 2020 Sep 9;2020.09.09.288555.

596 65. Horwitz, Bar-On Y, Lu C-L, Fera D, Lockhart AAK, Lorenzi JCC, et al. Non-

597 neutralizing Antibodies Alter the Course of HIV-1 Infection In Vivo. Cell. 2017 Jul 26;

598 66. Chung AW, Ghebremichael M, Robinson H, Brown E, Choi I, Lane S, et al.

599 Polyfunctional Fc-effector profiles mediated by IgG subclass selection distinguish RV144 and

600 VAX003 vaccines. Sci Transl Med. 2014 Mar 19;6(228):228ra38.

601 67. Ilinykh PA, Huang K, Santos RI, Gilchuk P, Gunn BM, Karim MM, et al. Non-

602 neutralizing Antibodies from a Marburg Infection Survivor Mediate Protection by Fc-Effector

603 Functions and by Enhancing Efficacy of Other Antibodies. Cell Host Microbe. 2020

604 10;27(6):976-991.e11.

605 68. Gunn BM, Yu W-H, Karim MM, Brannan JM, Herbert AS, Wec AZ, et al. A Role for Fc

606 Function in Therapeutic Monoclonal Antibody-Mediated Protection against Ebola Virus. Cell

607 Host Microbe. 2018 08;24(2):221-233.e5.

608 69. Zohar T, Alter G. Dissecting antibody-mediated protection against SARS-CoV-2. Nat

609 Rev Immunol. 2020;20(7):392–4.

610 70. Pinto D, Park Y-J, Beltramello M, Walls AC, Tortorici MA, Bianchi S, et al. Cross-

611 neutralization of SARS-CoV-2 by a human monoclonal SARS-CoV antibody. Nature.

612 2020;583(7815):290–5.

613 71. Natarajan H, Crowley AR, Butler SE, Xu S, Weiner JA, Bloch EM, et al. SARS-CoV-2

614 antibody signatures robustly predict diverse antiviral functions relevant for convalescent plasma

615 therapy. MedRxiv Prepr Serv Health Sci. 2020 Sep 18;

616 72. Atyeo C, Fischinger S, Zohar T, Slein MD, Burke J, Loos C, et al. Distinct Early

617 Serological Signatures Track with SARS-CoV-2 Survival. Immunity [Internet]. 2020 Jul 30

618 [cited 2020 Aug 12]; Available from:

619 http://www.sciencedirect.com/science/article/pii/S1074761320303277

620 73. Mercado NB, Zahn R, Wegmann F, Loos C, Chandrashekar A, Yu J, et al. Single-shot

621 Ad26 vaccine protects against SARS-CoV-2 in rhesus macaques. Nature. 2020 Jul 30;

622 74. Yu H-Q, Sun B-Q, Fang Z-F, Zhao J-C, Liu X-Y, Li Y-M, et al. Distinct features of

623 SARS-CoV-2-specific IgA response in COVID-19 patients. Eur Respir J. 2020;56(2).

624 75. Meyer-Bahlburg A. B-1 cells as a source of IgA. Ann N Y Acad Sci. 2015

625 Dec;1362:122–31.

626 76. Rodriguez-Zhurbenko N, Quach TD, Hopkins TJ, Rothstein TL, Hernandez AM. Human

627 B-1 Cells and B-1 Cell Antibodies Change With Advancing Age. Front Immunol [Internet].

628 2019 [cited 2020 Aug 6];10. Available from:

629 https://www.frontiersin.org/articles/10.3389/fimmu.2019.00483/full

630 77. Amanat F, Stadlbauer D, Strohmeier S, Nguyen THO, Chromikova V, McMahon M, et

631 al. A serological assay to detect SARS-CoV-2 seroconversion in humans. Nat Med. 2020 May

632 12;1–4.

633 78. Stadlbauer D, Amanat F, Chromikova V, Jiang K, Strohmeier S, Arunkumar GA, et al.

634 SARS-CoV-2 Seroconversion in Humans: A Detailed Protocol for a Serological Assay, Antigen

635 Production, and Test Setup. Curr Protoc Microbiol. 2020;57(1):e100.

636

637

Funding

This study was supported by the Microbiology Laboratory Clinical Services at the Mount Sinai Health System and the Mount Sinai Health System Translational Science Hub, National Institutes of Health [grant U54TR001433]; the Personalized Virology Initiative supported by institutional funds and philanthropic donations (to V.S.); the Department of Medicine of the Icahn School of Medicine at Mount Sinai Department of Medicine (to S.Z-P., C.E.H.); the Department of Microbiology and the Ward-Coleman estate for endowing the Ward-Coleman Chairs at the Icahn School of Medicine at Mount Sinai (to B.L.), the National Institute of Allergy and Infectious Diseases Centers of Excellence for Influenza Research and Surveillance [contract HHSN272201400008C] (to F.K., V.S.); the Department of Veterans Affairs [Merit Review Grant I01BX003860] (to C.E.H.) and [Research Career Scientist Award 1IK6BX004607] (to C.E.H.); the National Institute of Allergy and Infectious Diseases [grant AI139290] to C.E.H., [grant AI136916] (to V.S.), [grants R01 AI123449, R21 AI1498033] to B.L.
K.Y.O. and C.S. were supported by Viral-Host Pathogenesis Training Grant T32 AI07647; K.Y.O. was additionally supported by F31 AI154739. S.I. and C-T. H. were supported by postdoctoral fellowships from CHOT-SG (Fukuoka University, Japan) and the Ministry of Science and Technology (MOST, Taiwan), respectively.

Acknowledgments

We thank all the donors for their contribution to research.

Competing interests

660 The authors declare no competing interests.

661

662 ## Author contributions

663 J.K., S.W., G.E-A., S.Z-P., and C.E.H. wrote and edited the manuscript. S.W., J.K., C.E.H., and
664 S.Z-P. designed the experiments. J.K., S.W., V.I., X.L. performed the experiments and collected
665 the data. J.K., A.N., S.Z-P. and C.E.H. analyzed the data. K.Y.O., C.S., S.I., C-T.H., F.A., B.L.,
666 and F.K. provided protocols, antigens, cells and pseudovirus stocks. G.E-A., I.B., S.A., J.C.B.,
667 E.M.K., J.S., S.L., D.J., M.B-G., and V.S. provided samples. All authors read and approved the
668 final manuscript.

669

Figure legends

Fig. 1. Titration of SARS-CoV-2 spike and RBD total Ig in plasma or serum samples from COVID-19 convalescent individuals. Titration of (a) spike-specific or (b) RBD-specific total Ig from 29 COVID-19-convalescent individuals, two acute COVID-19 patients with longitudinal samples, and 13 COVID-19-negative individuals. Specimens were diluted at 2-fold dilutions from 1:50 to 1:6,400.

Fig. 2. Levels of Ig isotypes against the SARS-CoV-2 spike and RBD vary in plasma or serum samples from COVID-19 convalescent individuals. Detection of total Ig, IgM, IgG1, IgG2, IgG3, IgG4, IgA1 and IgA2 against (a) spike and (b) RBD in specimens from 29 COVID-19-convalescent individuals, 13 COVID-19-negative contemporary samples, and pre-pandemic controls. The samples were tested at a dilution of 1:200 and data are shown as mean MFI + standard deviation (SD) of duplicate measurements from at least two independent experiments. The pre-pandemic controls are shown as mean MFI + SD of 12 samples (Pre, black bar). The horizontal red dotted line represents the cut-off value determined as the mean + 3 SD of 12 pre-pandemic samples for each of the isotypes. (c) Percentages of responders above the cut-off for each spike- or RBD-specific Ig isotype.

Fig. 3. IgG1 is the dominant isotype response induced in COVID-19 convalescent individuals. Simple linear regression of (a) spike-specific or (b) RBD-specific total Ig levels versus IgM, IgG1 or IgG2 levels or versus (c) spike-specific and RBD-specific IgG3, IgG4, IgA1, and IgA2 levels from the 29 COVID-19-convalescent individuals from Fig. 1. The dash lines represent 95% confidence intervals.

Fig. 4. Neutralization activities are detected in all COVID-19 convalescent individuals. Neutralization of COV2pp with (a,b,c) WT or (d,e) D614G mutated spike proteins by samples

693 from (a,d) 28 COVID-19-convalescent individuals and (b,e) 11 COVID-19-negative individuals,
694 compared to (c) a recombinant soluble RBD (sRBD) control. Each plasma or sera specimen was
695 tested at 4-fold dilutions from 1:10 to 1:40,960, and sRBD was tested at 4-fold dilutions from
696 100 to 0.02 µg/mL. The data are shown as mean percentage of neutralization + SD of triplicate.
697 The extrapolated titration curves were generated using a nonlinear regression model in GraphPad
698 Prism (Inhibitor versus response – variable slope (four parameters), least squares regression).
699 The dotted horizontal lines highlight 50% neutralization. (f) Spearman correlation between the
700 IC_{90} titers against COV2pp WT versus D614G.

701 **Fig. 5. Summary of relative Ig isotype levels and neutralization titers.** Table showing sex
702 (purple, F: female, M: male), relative levels of spike-specific (green) and RBD-specific (blue) Ig
703 isotypes (+: bottom quartile, ++: second quartile, +++: third quartile, ++++: top quartile, -: non-
704 responder) and reciprocal IC_{50} and IC_{90} neutralization titers against WT pseudovirus (orange)
705 and D614G pseudovirus (red) of 29 plasma samples from COVID-19-convalescent individuals
706 (nd: not done).

707 **Fig. 6. IgM and IgG1 contribute most to SARS-CoV-2 neutralization.** Simple linear
708 regression of reciprocal IC_{90} neutralization titers of 27 COVID-19-convalescent individuals
709 versus (a) spike-specific or (b) RBD-specific total Ig, IgM, IgG1 and IgA1 Ab levels. The black
710 dash line shows 95% confidence interval. The dotted vertical red line represents the cut-off
711 (mean of 12 pre-pandemic samples + 3 SD) for each isotype from Fig. 1. (b) Simple linear
712 regression of reciprocal IC_{90} neutralization titers of 27 COVID-19-convalescent individuals
713 versus spike-specific or RBD-specific total IgG2-4 and IgA2 Ab levels.

714 **Fig. 7. Purified IgM, IgG, and IgA fractions display neutralizing activities against SARS-**
715 **CoV-2.** (a) Neutralization of COV2pp by five COVID-19-infected individual plasma samples

(RP#1-5) compared to a COVID-19-negative sample (RN#1). Plasma samples were tested at 4-fold dilutions from 1:10 to 1:40,960 or 1:20 to 1:81,920. Data are shown as the mean percentage of neutralization. The dotted horizontal lines highlight 50% neutralization. (b) Reciprocal IC_{50} and IC_{90} neutralization titers of RP#1-5 plasma samples (c) Neutralization of COV2pp by purified IgM, IgG, and IgA fractions from five COVID-19-infected individuals (RP#1-5) compared to a control Ig fraction. The fractions were tested at 4-fold dilutions from 500 to 0.02 µg/mL. Data are shown as the mean percentage of neutralization. The dotted horizontal lines highlight 50% neutralization. (d) IC_{50} of purified IgM, IgG, and IgA fractions from RP#1-5. The statistical significance was determined by a two-tailed Mann-Whitney test (*: $p < 0.05$, **: $p < 0.01$).

Supplementary Fig. 1. Spearman correlations of (a) spike-specific or (b) RBD-specific total Ig MFI values from two independent experiments to show the degree of assay reproducibility.

Supplementary Fig. 2. Spearman correlations of the area under the curves (AUCs) of (a) spike- or (b) RBD-specific total Ig versus total Ig MFI values at a 1:200 dilution.

Supplementary Fig. 3. Isotyping validation was performed by coating Luminex beads with IgG1, IgG2, IgG3, IgG4, IgA1, IgA2, and IgM myeloma proteins and detecting each specifically with eight different secondary Abs against (a) total Ig, (b) IgM, (c) IgG1, (d) IgG2, (e) IgG3, (f) IgG4, (g) IgA1 and (h) IgA2. The data are shown as mean MFI + SD of duplicate.

Supplementary Fig. 4. Spearman correlations between spike-specific versus RBD-specific total Ig, IgM, IgG1, IgG2, IgG3, IgG4, IgA1, or IgA2 MFI values.

Supplementary Fig. 5. Violin plots of (a) spike-specific or (b) RBD-specific total Ig, IgM, IgG1, and IgA1 levels from nine COVID-19 convalescent female (F) and 15 male (M) subjects.

739 The statistical significance was determined by a two-tailed Mann-Whitney test (ns: non-
740 significant: $p > 0.05$).

741 **Supplementary Fig. 6. Induction of IgA1 and IgG1 along with IgM early after disease**
742 **onset**. Kinetics of induction of spike-specific (left panel) or RBD-specific (right panel) (a) total
743 Ig, (b) IgM, (c) IgG1, (d) IgG2, (e) IgG3, (f) IgG4, (g) IgA1, and (h) IgA2 from two COVID-19
744 patients. Longitudinal samples from each patient were tested at a dilution of 1:200 in parallel
745 with all negative samples and data are shown as mean MFI + SD of duplicate measurements
746 from at least two experiments. The dotted red line represents the cut-off value calculated as the
747 mean of 12 pre-pandemic samples + 3 SD from Fig. 1.

748 **Supplementary Fig. 7. Enrichment of spike-specific (a) IgM, (b) IgG, and (c) IgA in**
749 **purified fractions from RP#1-5 and RN#1.** Each fraction was measured for the presence of
750 IgM, IgG1, IgG2, IgG3, IgG4, IgA1, and IgA2 Abs using the isotyping method validated in
751 Supplementary Fig. 3.

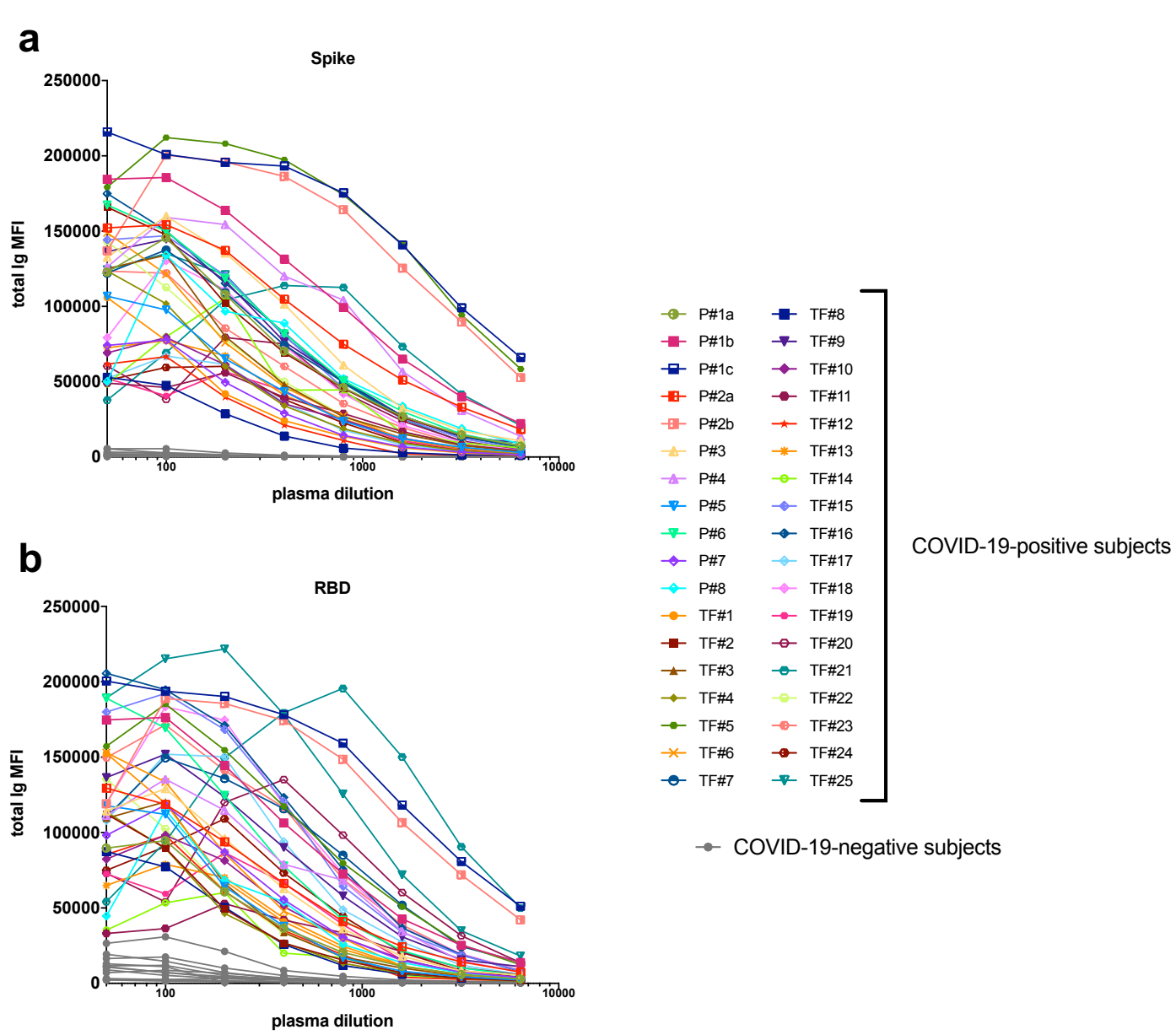
a
Spike
250000
200000
150000
100000
50000
0
total Ig MFI
100
1000
10000
plasma dilution
b
RBD
250000
200000
150000
100000
50000
0
total Ig MFI
100
1000
10000
plasma dilution
P#1a
P#1b
P#1c
P#2a
P#2b
P#3
P#4
P#5
P#6
P#7
P#8
TF#1
TF#2
TF#3
TF#4
TF#5
TF#6
TF#7
TF#8
TF#9
TF#10
TF#11
TF#12
TF#13
TF#14
TF#15
TF#16
TF#17
TF#18
TF#19
TF#20
TF#21
TF#22
TF#23
TF#24
TF#25
COVID-19-positive subjects
COVID-19-negative subjects

Fig. 1. Titration of SARS-CoV-2 spike and RBD total Ig in plasma or serum samples from COVID-19 convalescent individuals. Titration of (a) spike-specific or (b) RBD-specific total Ig from 29 COVID-19-convalescent individuals, two acute COVID-19 patients with longitudinal samples, and 13 COVID-19-negative individuals. Specimens were diluted at 2-fold dilutions from 1:50 to 1:6,400.

a

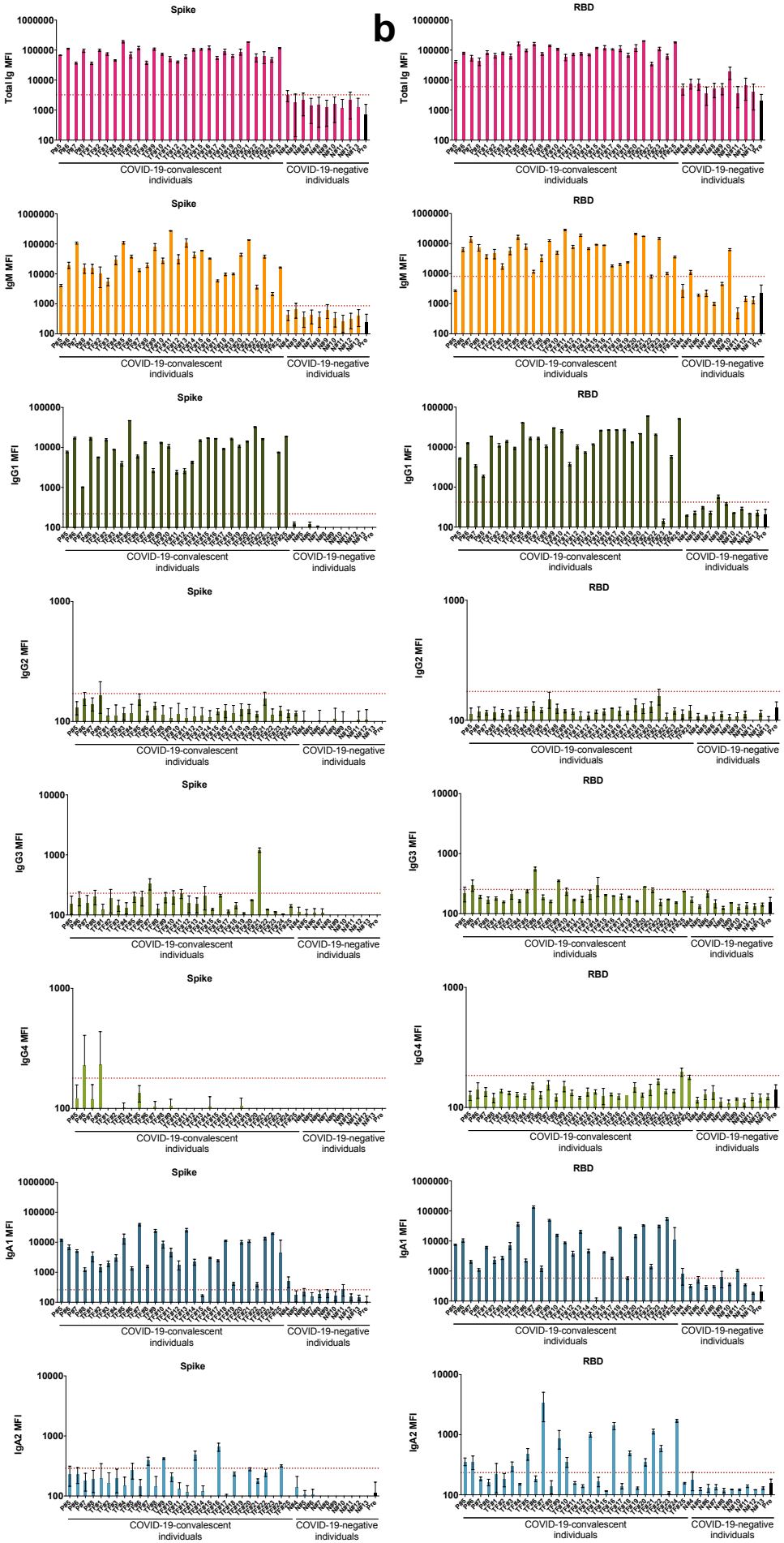

b

c

	Spike	RBD
Total Ig	100%	100%
IgM	100%	93%
IgG1	97%	97%
IgG2	0%	0%
IgG3	7%	17%
IgG4	7%	3%
IgA1	97%	93%
IgA2	17%	48%

Fig. 2. Levels of Ig isotypes against the SARS-CoV-2 spike and RBD vary in plasma or serum samples from COVID-19 convalescent individuals. Detection of total Ig, IgM, IgG1, IgG2, IgG3, IgG4, IgA1 and IgA2 against (a) spike and (b) RBD in specimens from 29 COVID-19-convalescent individuals, 13 COVID-19-negative contemporary samples, and pre-pandemic controls. The samples were tested at a dilution of 1:200 and data are shown as mean MFI + standard deviation (SD) of duplicate measurements from at least two independent experiments. The pre-pandemic controls are shown as mean MFI + SD of 12 samples (Pre, black bar). The horizontal red dotted line represents the cut-off value determined as the mean + 3 SD of 12 pre-pandemic samples for each of the isotypes. (c) Percentages of responders above the cut-off for each spike- or RBD-specific Ig isotype.

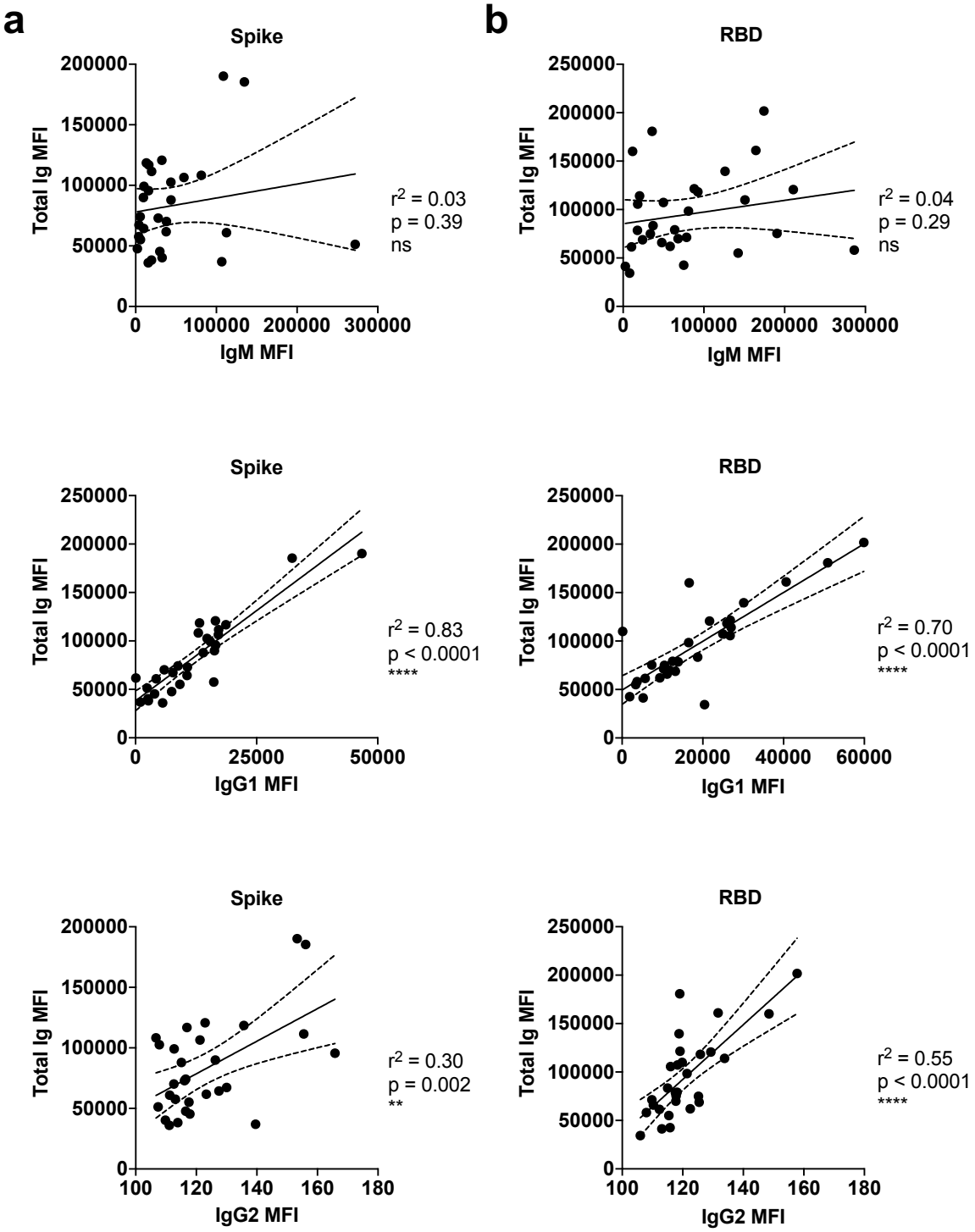

c

	Linear regression spike MFI			Linear regression RBD MFI		
	r^2	p		r^2	p	
Total vs IgG3	0.35	0.0008	***	0.07	0.15	ns
Total vs IgG4	0.07	0.15	ns	0.24	0.007	¨**
Total vs IgA1	0.06	0.20	ns	0.23	0.009	***
Total vs IgA2	0.06	0.20	ns	0.13	0.05	ns

Fig. 3. IgG1 is the dominant isotype response induced in COVID-19 convalescent individuals. Simple linear regression of (a) spike-specific or (b) RBD-specific total Ig levels versus IgM, IgG1 or IgG2 levels or versus (c) spike-specific and RBD-specific IgG3, IgG4, IgA1, and IgA2 levels from the 29 COVID-19-convalescent individuals from Fig. 1. The dash lines represent 95% confidence intervals.

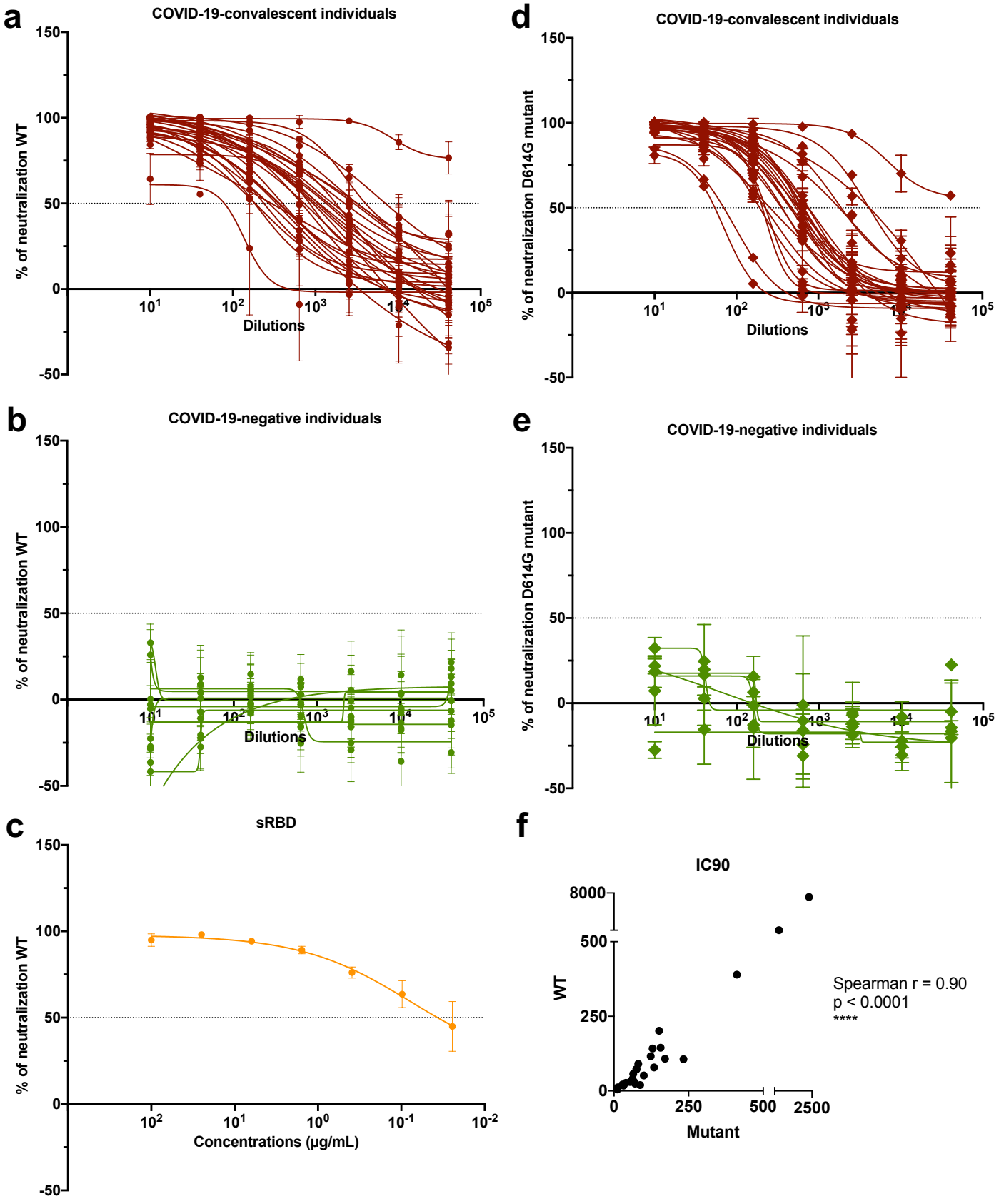
a
COVID-19-convalescent individuals
% of neutralization WT
Dilutions
d
COVID-19-convalescent individuals
% of neutralization D614G mutant
Dilutions
b
COVID-19-negative individuals
% of neutralization WT
Dilutions
e
COVID-19-negative individuals
% of neutralization D614G mutant
Dilutions
c
sRBD
% of neutralization WT
Concentrations (µg/mL)
f
IC90
WT
Mutant
Spearman r = 0.90
p < 0.0001
****

Fig. 4. Neutralization activities are detected in all COVID-19 convalescent individuals. Neutralization of COV2pp with (a,b,c) WT or (d,e) D614G mutated spike proteins by samples from (a,d) 28 COVID-19-convalescent individuals and (b,e) 11 COVID-19-negative individuals, compared to (c) a recombinant soluble RBD (sRBD) control. Each plasma or sera specimen was tested at 4-fold dilutions from 1:10 to 1:40,960, and sRBD was tested at 4-fold dilutions from 100 to 0.02 µg/mL. The data are shown as mean percentage of neutralization + SD of triplicate. The extrapolated titration curves were generated using a nonlinear regression model in GraphPad Prism (Inhibitor versus response – variable slope (four parameters), least squares regression). The dotted horizontal lines highlight 50% neutralization. (f) Spearman correlation between the IC_{90} titers against COV2pp WT versus D614G.

	Sex	Spike								RBD								Neutralization		Neutralization D614G mutant	
		Total Ig	IgM	IgG1	IgG2	IgG3	IgG4	IgA1	IgA2	Total Ig	IgM	IgG1	IgG2	IgG3	IgG4	IgA1	IgA2	IC_{50}	IC_{90}	IC_{50}	IC_{90}
P#5	unknown	++	+	+	-	-	-	++	-	+	-	+	-	-	-	+	+	36.6	2.3	nd	nd
P#6	unknown	+++	+	++	-	-	+	+	-	++	+	+	-	+	-	+	+	561.0	25.6	nd	nd
P#7	unknown	+	++	+	-	-	-	+	-	++	++	+	-	-	-	+	-	nd	nd	nd	nd
P#8	unknown	++	+	++	-	-	+	+	-	+	++	+	-	-	-	+	-	376.2	10.2	nd	nd
TF#1	F	+	+	+	-	-	-	+	-	++	+	++	-	-	-	+	-	418.8	21.5	254.8	28.6
TF#2	M	++	+	++	-	-	-	+	-	++	+	+	-	-	-	+	-	177.5	11.8	59.6	12.7
TF#3	M	++	+	+	-	-	-	+	-	++	+	+	-	-	-	+	+	164.7	19.8	206.2	87.5
TF#4	F	+	+	+	-	-	-	+	-	++	+	+	-	-	-	+	-	998.6	39.9	328.7	62.1
TF#5	M	++++	++	++++	-	-	-	++	-	++++	+++	+++	-	-	-	++	+	2344.7	515.9	4138.0	730.1
TF#6	F	++	+	+	-	-	-	+	-	++	+	++	-	+	-	+	-	976.6	51.9	551.8	99.7
TF#7	F	+++	+	++	-	+	-	++++	+	++++	+	++	-	-	-	++++	+	5788.5	90.7	452.5	81.2
TF#8	M	+	+	+	-	-	-	+	-	++	+	+	-	-	-	+	-	2840.0	142.1	700.1	129.1
TF#9	F	+++	++	++	-	-	-	+++	+	+++	++	++	-	+	-	++	+	4044.1	116.5	664.2	122.8
TF#10	M	++	+	+	-	-	-	+	-	+++	+	++	-	-	-	+	+	1060.0	72.7	572.1	75.0
TF#11	M	++	++++	+	-	-	-	+	-	++	++++	+	-	-	-	+	-	> 40960	7200.0	> 40960	2344.0
TF#12	F	+	+	+	-	-	-	+	-	++	++	+	-	-	-	+	-	285.5	30.0	325.7	54.12
TF#13	M	++	++	+	-	-	-	+++	+	++	+++	+	-	-	-	+	+	1697.6	144.9	1573.0	156.1
TF#14	M	+++	+	++	-	-	-	+	-	++	+	+	-	+	-	+	-	17078.5	201.4	675.2	151.1
TF#15	M	+++	+	++	-	-	-	-	-	+++	++	++	-	-	-	-	-	2006.2	29.6	548.5	67.9
TF#16	M	+++	+	++	-	-	-	+	+	+++	++	++	-	-	-	+	+	1330.7	106.2	1961.0	233.0
TF#17	M	++	+	+	-	-	-	+	-	+++	+	++	-	-	-	+	-	198.0	27.2	185.9	39.8
TF#18	F	++	+	++	-	-	-	++	-	+++	+	++	-	-	-	+	+	1122.1	56.9	453.8	64.4
TF#19	M	++	+	+	-	-	-	+	-	++	+	+	-	-	-	-	-	326.2	17.7	201.4	31.8
TF#20	F	++	+	++	-	-	-	++	-	+++	+++	++	-	+	-	+	+	1535.3	72.4	471.0	75.5
TF#21	M	++++	++	+++	-	+	-	++	-	++++	+++	++++	-	-	-	+	+	5375.7	389.7	3231.0	411.8
TF#22	M	++	+	++	-	-	-	+	-	+	-	++	-	-	-	+	+	623.2	4.8	46.65	11.5
TF#23	unknown	++	+	-	-	-	-	++	-	+++	+++	-	-	-	-	+	-	3881.9	107.8	563.7	170.9
TF#24	M	+	+	+	-	-	-	++	+	++	+	+	-	-	+	++	+	813.6	24.4	214.8	70.7
TF#25	F	+++	+	++	-	-	-	+	-	++++	+	++++	-	-	-	+	-	958.6	78.7	605.0	134.0

Fig. 5. Summary of relative Ig isotype levels and neutralization titers. Table showing sex (purple, F: female, M: male), relative levels of spike-specific (green) and RBD-specific (blue) Ig isotypes (+: bottom quartile, ++: second quartile, +++: third quartile, ++++: top quartile, -: non-responder) and reciprocal IC_{50} and IC_{90} neutralization titers against WT pseudovirus (orange) and D614G pseudovirus (red) of 29 plasma samples from COVID-19-convalescent individuals (nd: not done).

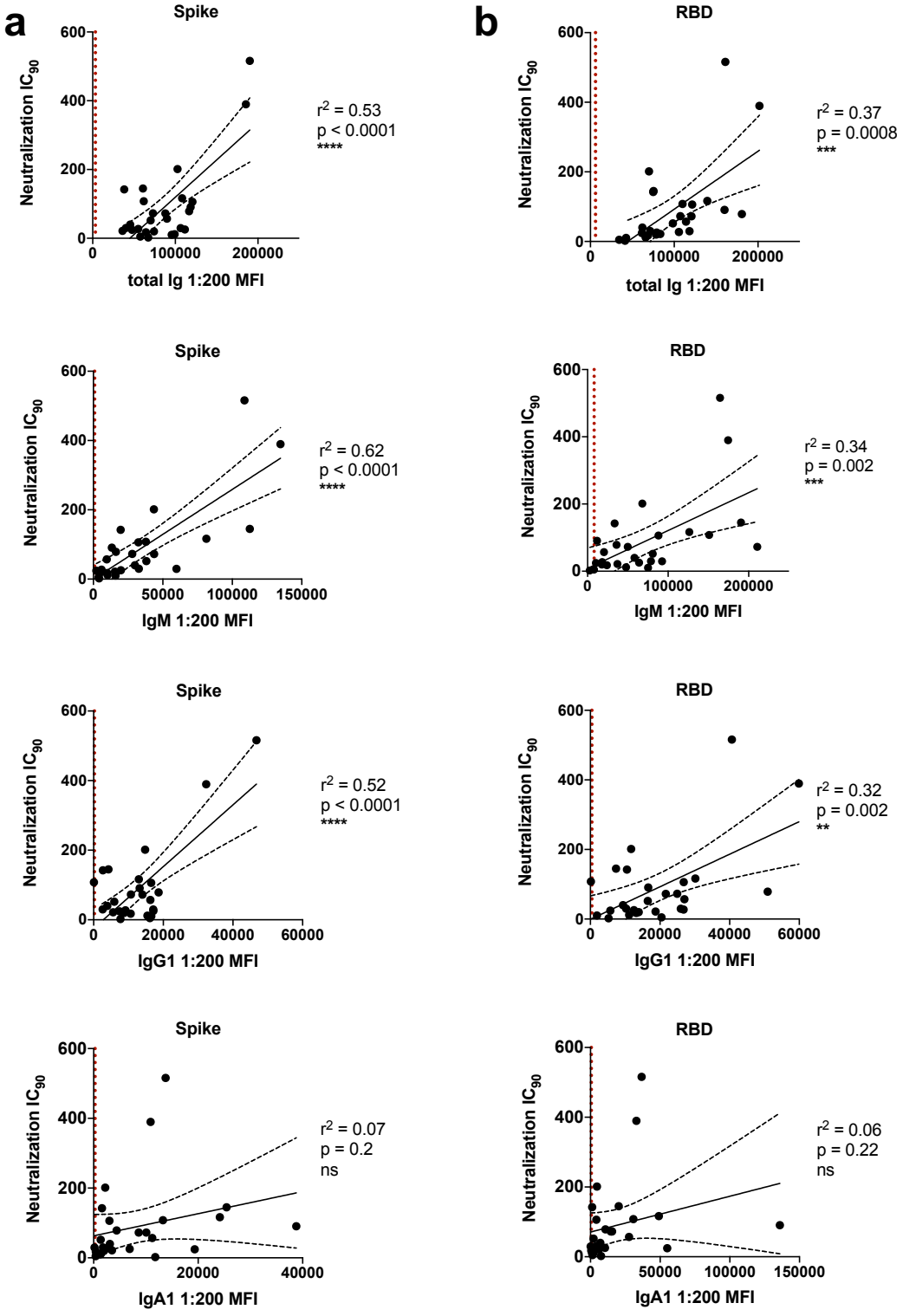

c

	Linear regression IC_{90} versus Spike MFI			Linear regression IC_{90} versus RBD MFI		
	r^2	p		r^2	p	
IgG2	0.14	0.05	ns	0.33	0.002	**
IgG3	0.30	0.003	**	0.02	0.46	ns
IgG4	0.00	0.99	ns	0.06	0.21	ns
IgA2	0.02	0.50	ns	0.03	0.45	ns

Fig. 6. IgM and IgG1 contribute most to SARS-CoV-2 neutralization. Simple linear regression of reciprocal IC_{90} neutralization titers of 27 COVID-19-convalescent individuals versus (a) spike-specific or (b) RBD-specific total Ig, IgM, IgG1 and IgA1 Ab levels. The black dash line shows 95% confidence interval. The dotted vertical red line represents the cut-off (mean of 12 pre-pandemic samples + 3 SD) for each isotype from Fig. 1. (b) Simple linear regression of reciprocal IC_{90} neutralization titers of 27 COVID-19-convalescent individuals versus spike-specific or RBD-specific total IgG2-4 and IgA2 Ab levels.

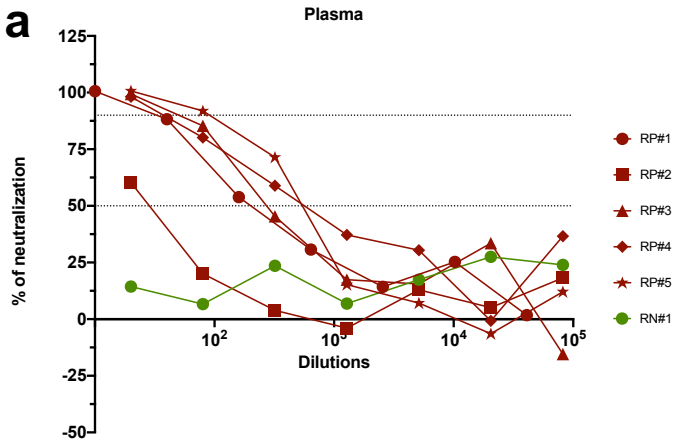

b

	Neutralization	
	IC_{50}	IC_{90}
RP#1	240	35
RP#2	35	< 20
RP#3	290	60
RP#4	690	45
RP#5	690	100

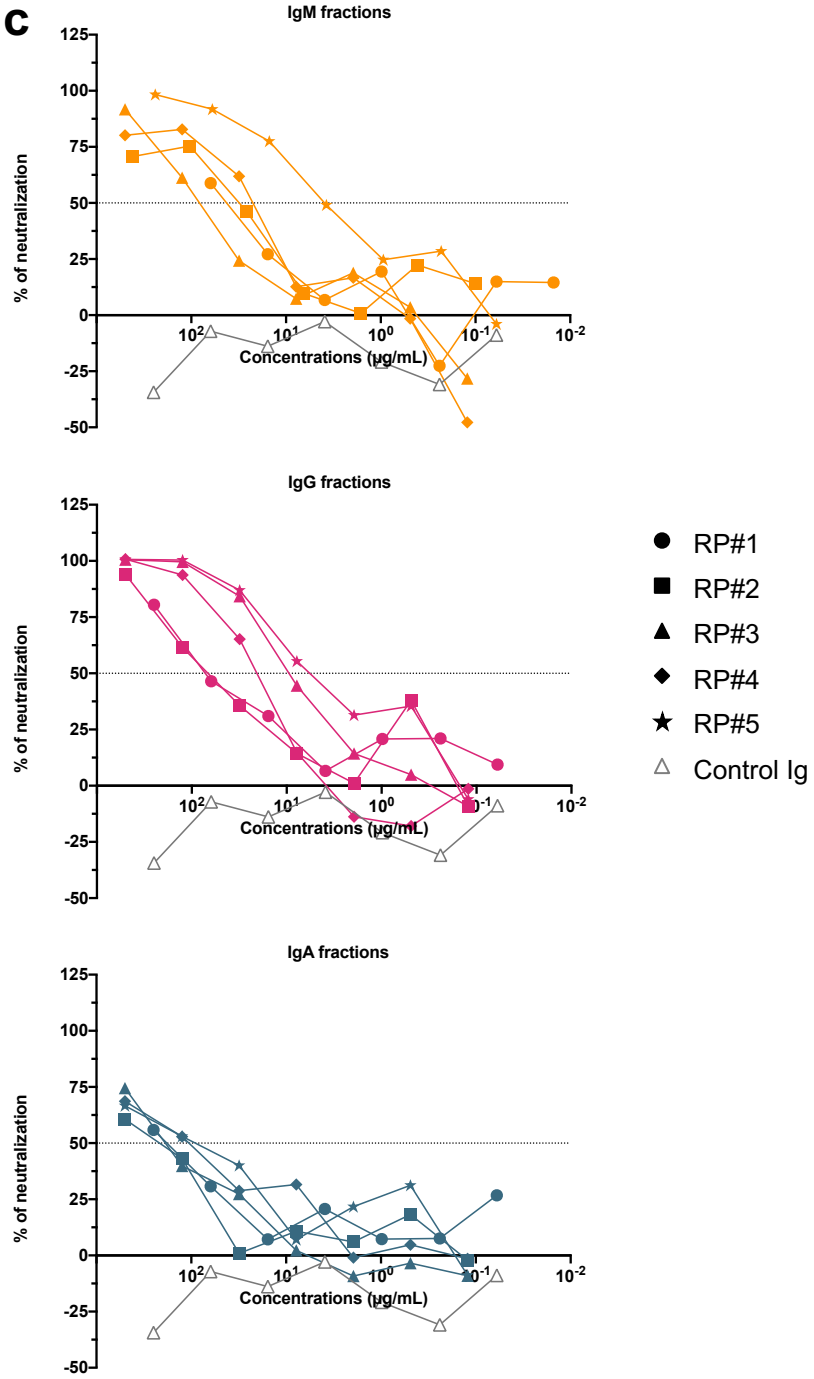

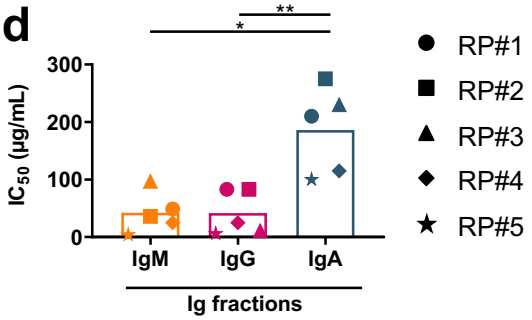

Fig. 7. Purified IgM, IgG, and IgA fractions display neutralizing activities against SARS-CoV-2. (a) Neutralization of COV2pp by five COVID-19-infected individual plasma samples (RP#1-5) compared to a COVID-19-negative sample (RN#1). Plasma samples were tested at 4-fold dilutions from 1:10 to 1:40,960 or 1:20 to 1:81,920. Data are shown as the mean percentage of neutralization. The dotted horizontal lines highlight 50% neutralization. (b) Reciprocal IC_{50} and IC_{90} neutralization titers of RP#1-5 plasma samples (c) Neutralization of COV2pp by purified IgM, IgG, and IgA fractions from five COVID-19-infected individuals (RP#1-5) compared to a control Ig fraction. The fractions were tested at 4-fold dilutions from 500 to 0.02 μg/mL. Data are shown as the mean percentage of neutralization. The dotted horizontal lines highlight 50% neutralization. (d) IC_{50} of purified IgM, IgG, and IgA fractions from RP#1-5. The statistical significance was determined by a two-tailed Mann-Whitney test (*: $p < 0.05$, **: $p < 0.01$).

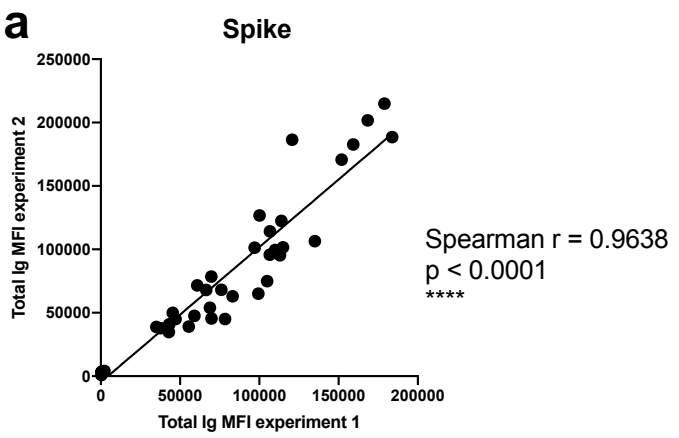
a
Spike
Total Ig MFI experiment 2
Total Ig MFI experiment 1
0
50000
100000
150000
200000
250000
Spearman r = 0.9638
p < 0.0001
****

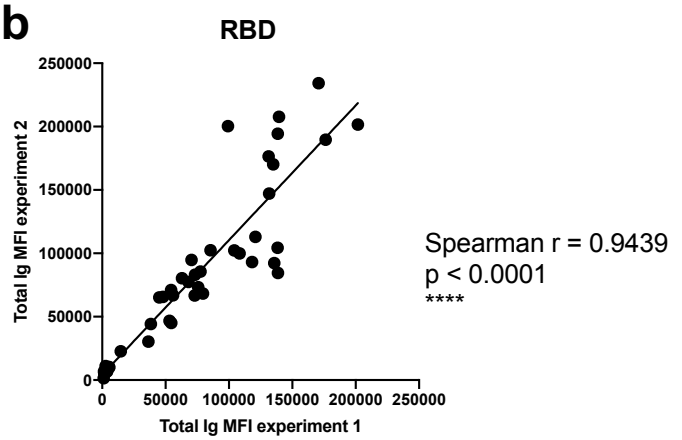
b
RBD
Total Ig MFI experiment 2
Total Ig MFI experiment 1
0
50000
100000
150000
200000
250000
Spearman r = 0.9439
p < 0.0001
****

Supplementary Fig. 1. Spearman correlations of (a) spike-specific or (b) RBD-specific total Ig MFI values from two independent experiments to show the degree of assay reproducibility.

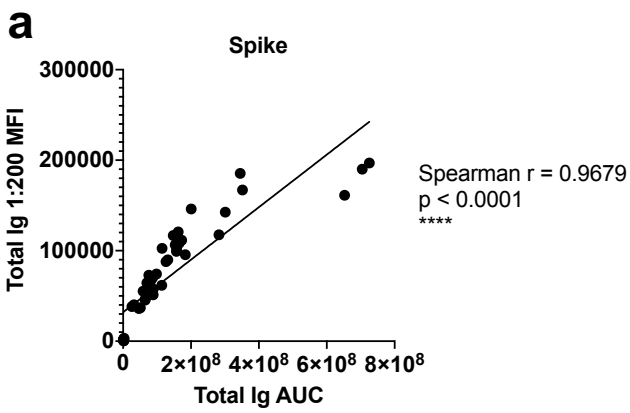
a
Spike
Total Ig 1:200 MFI
300000
200000
100000
0
0
2×10^8 4×10^8 6×10^8 8×10^8
Total Ig AUC
Spearman r = 0.9679
p < 0.0001
****

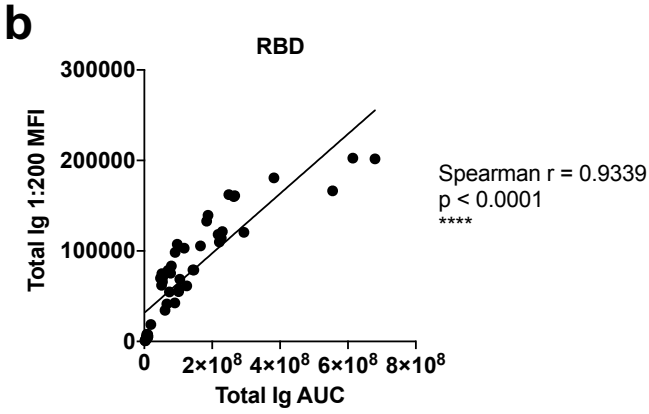
b
RBD
Total Ig 1:200 MFI
300000
200000
100000
0
0
2×10^8 4×10^8 6×10^8 8×10^8
Total Ig AUC
Spearman r = 0.9339
p < 0.0001
****

Supplementary Fig. 2. Spearman correlations of the area under the curves (AUCs) of (a) spike- or (b) RBD-specific total Ig versus total Ig MFI values at a 1:200 dilution.

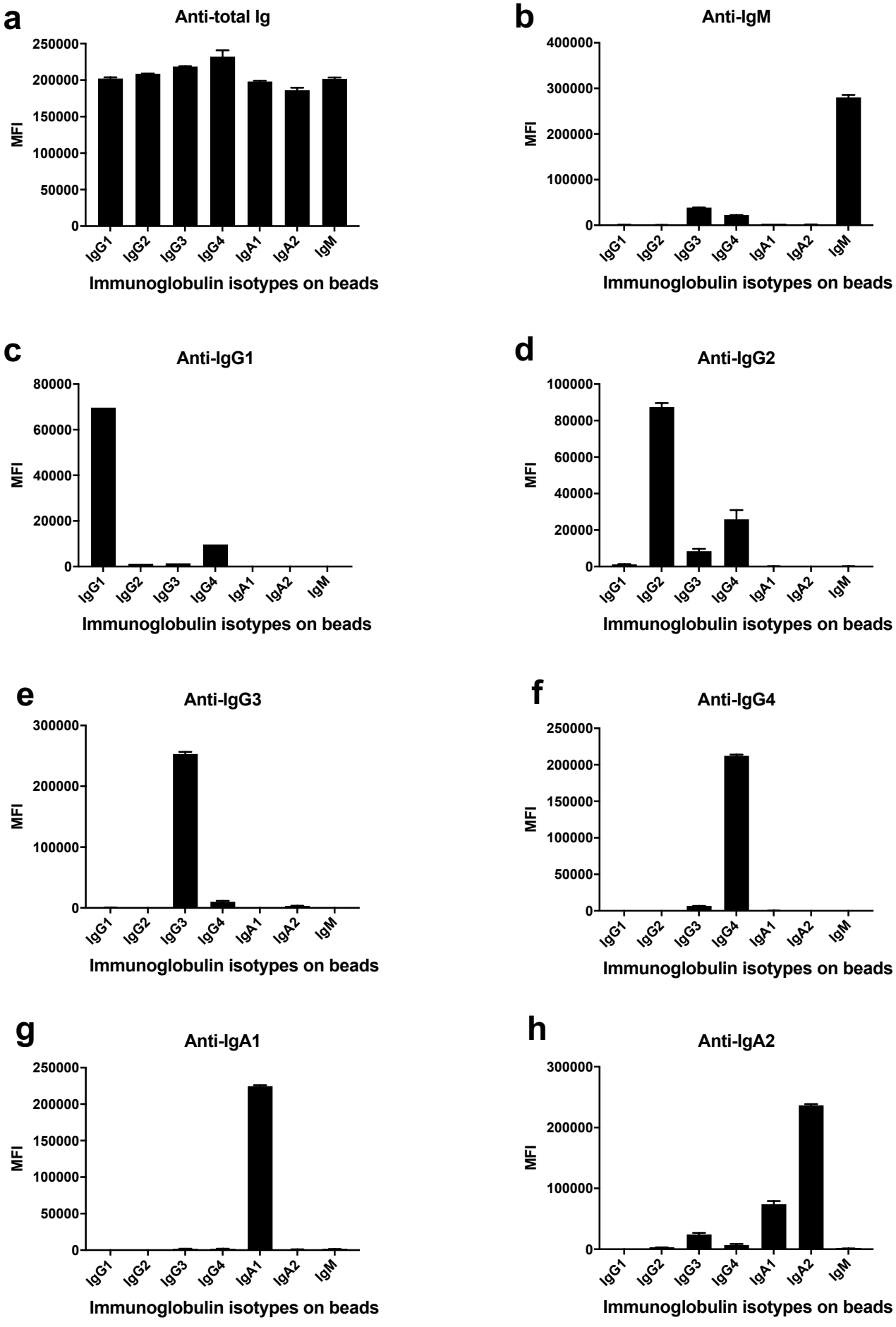
a
Anti-total Ig
MFI
250000
200000
150000
100000
50000
0
IgG1
IgG2
IgG3
IgG4
IgA1
IgA2
IgM
Immunoglobulin isotypes on beads
b
Anti-IgM
MFI
400000
300000
200000
100000
0
IgG1
IgG2
IgG3
IgG4
IgA1
IgA2
IgM
Immunoglobulin isotypes on beads
c
Anti-IgG1
MFI
80000
60000
40000
20000
0
IgG1
IgG2
IgG3
IgG4
IgA1
IgA2
IgM
Immunoglobulin isotypes on beads
d
Anti-IgG2
MFI
100000
80000
60000
40000
20000
0
IgG1
IgG2
IgG3
IgG4
IgA1
IgA2
IgM
Immunoglobulin isotypes on beads
e
Anti-IgG3
MFI
300000
200000
100000
0
IgG1
IgG2
IgG3
IgG4
IgA1
IgA2
IgM
Immunoglobulin isotypes on beads
f
Anti-IgG4
MFI
250000
200000
150000
100000
50000
0
IgG1
IgG2
IgG3
IgG4
IgA1
IgA2
IgM
Immunoglobulin isotypes on beads
g
Anti-IgA1
MFI
250000
200000
150000
100000
50000
0
IgG1
IgG2
IgG3
IgG4
IgA1
IgA2
IgM
Immunoglobulin isotypes on beads
h
Anti-IgA2
MFI
300000
200000
100000
0
IgG1
IgG2
IgG3
IgG4
IgA1
IgA2
IgM
Immunoglobulin isotypes on beads

Supplementary Fig. 3. Isotyping validation was performed by coating Luminex beads with IgG1, IgG2, IgG3, IgG4, IgA1, IgA2, and IgM myeloma proteins and detecting each specifically with eight different secondary Abs against (a) total Ig, (b) IgM, (c) IgG1, (d) IgG2, (e) IgG3, (f) IgG4, (g) IgA1 and (h) IgA2. The data are shown as mean MFI + SD of duplicate.

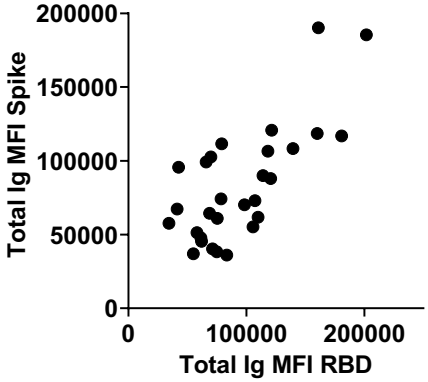

Spearman r = 0.6419
p = 0.0002
***

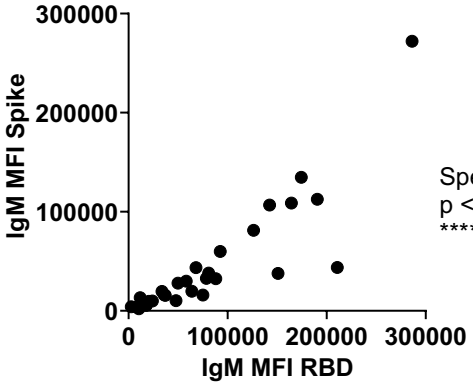

Spearman r = 0.9429
p < 0.0001
****

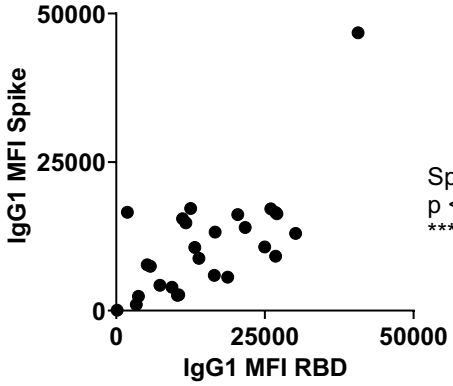

Spearman r = 0.6754
p < 0.0001
****

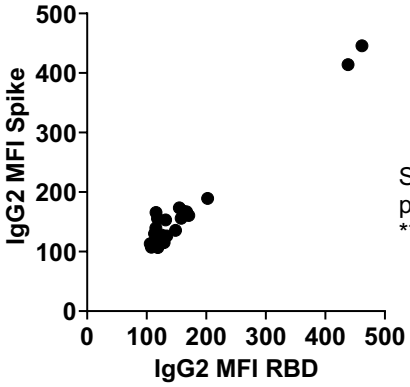

Spearman r = 0.6899
p < 0.0001
****

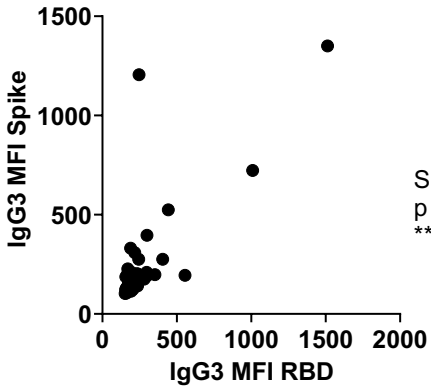

Spearman r = 0.6453
p < 0.0001
****

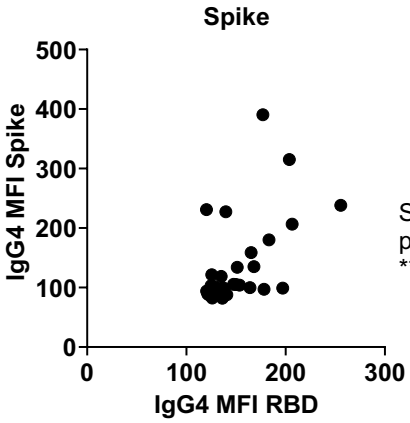

Spearman r = 0.5546
p = 0.0004
***

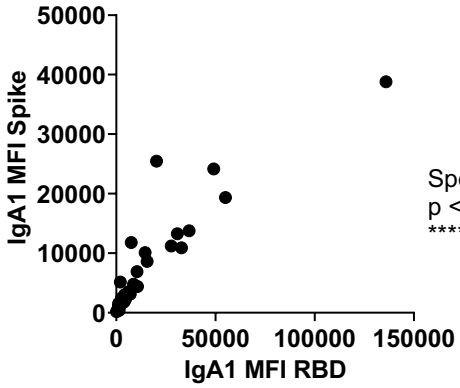

Spearman r = 0.9251
p < 0.0001
****

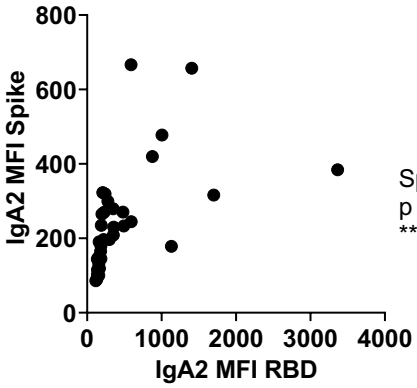

Spearman r = 0.8219
p < 0.0001
****

Supplementary Fig. 4. Spearman correlations between spike-specific versus RBD-specific total Ig, IgM, IgG1, IgG2, IgG3, IgG4, IgA1, or IgA2 MFI values.

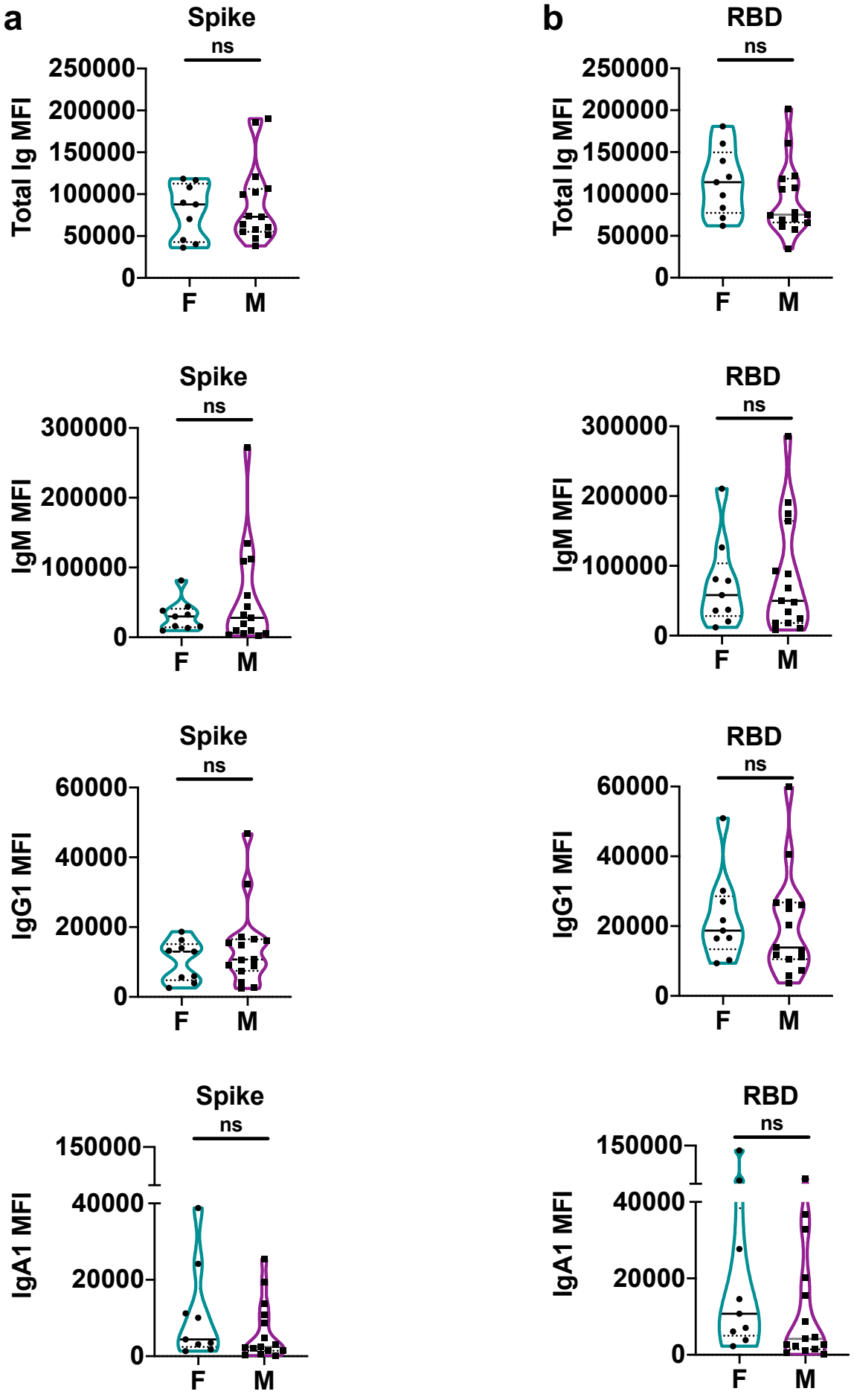
a
Spike
ns
Total Ig MFI
250000
200000
150000
100000
50000
0
F
M
b
RBD
ns
Total Ig MFI
250000
200000
150000
100000
50000
0
F
M
Spike
ns
IgM MFI
300000
200000
100000
0
F
M
RBD
ns
IgM MFI
300000
200000
100000
0
F
M
Spike
ns
IgG1 MFI
60000
40000
20000
0
F
M
RBD
ns
IgG1 MFI
60000
40000
20000
0
F
M
Spike
ns
IgA1 MFI
150000
40000
20000
0
F
M
RBD
ns
IgA1 MFI
150000
40000
20000
0
F
M

Supplementary Fig. 5. Violin plots of (a) spike-specific or (b) RBD-specific total Ig, IgM, IgG1, and IgA1 levels from nine COVID-19 convalescent female (F) and 15 male (M) subjects. The statistical significance was determined by a two-tailed Mann-Whitney test (ns: non-significant: $p > 0.05$).

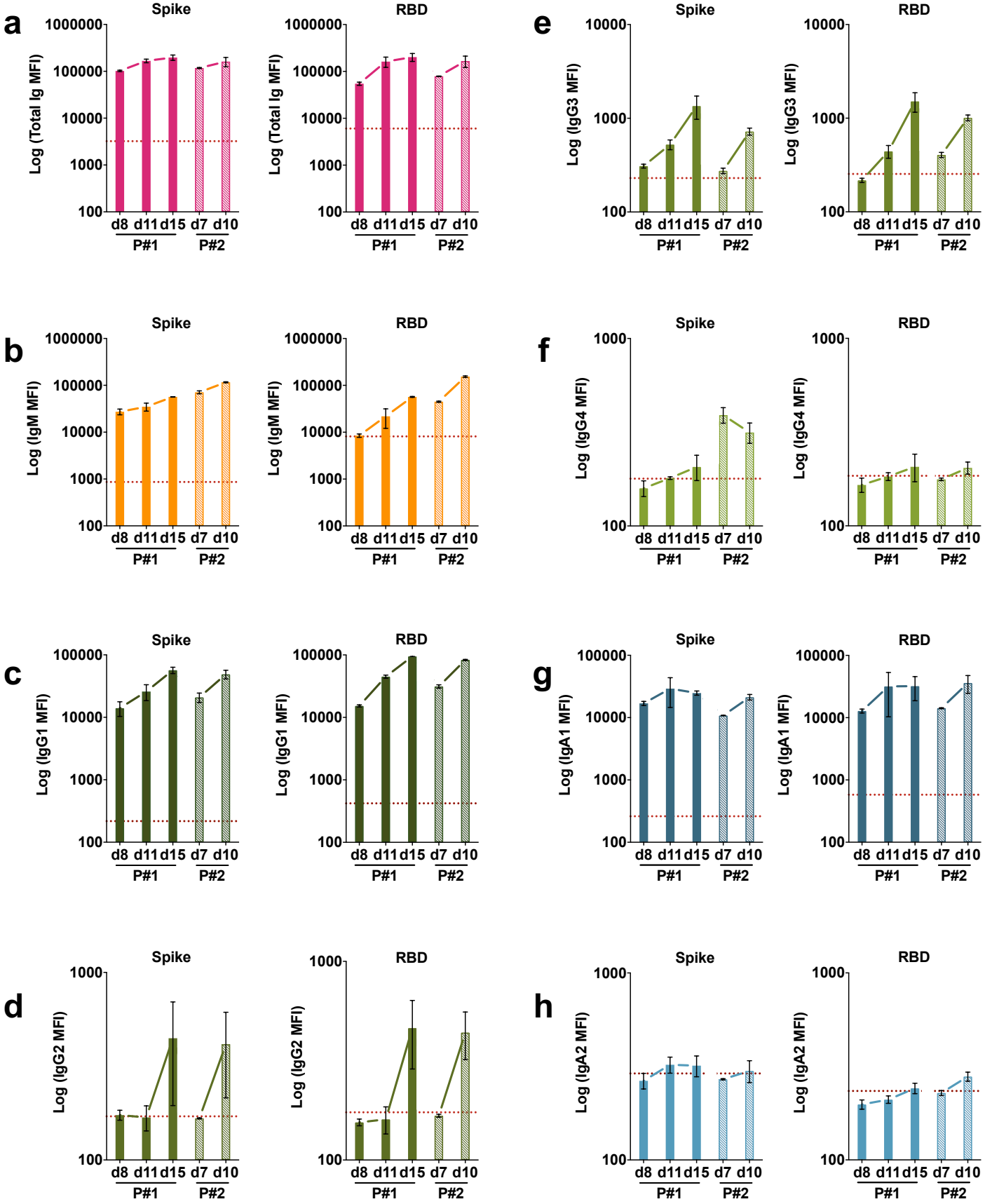
a
Spike
RBD
Log (Total Ig MFI)
1000000
100000
10000
1000
100
d8 d11 d15 d7 d10
P#1
P#2
b
Log (IgM MFI)
c
Log (IgG1 MFI)
d
Log (IgG2 MFI)
e
Log (IgG3 MFI)
f
Log (IgG4 MFI)
g
Log (IgA1 MFI)
h
Log (IgA2 MFI)

Supplementary Fig. 6. Induction of IgA1 and IgG1 along with IgM early after disease onset. Kinetics of induction of spike-specific (left panel) or RBD-specific (right panel) (a) total Ig, (b) IgM, (c) IgG1, (d) IgG2, (e) IgG3, (f) IgG4, (g) IgA1, and (h) IgA2 from two COVID-19 patients. Longitudinal samples from each patient were tested at a dilution of 1:200 in parallel with all negative samples and data are shown as mean MFI + SD of duplicate measurements from at least two experiments. The dotted red line represents the cut-off value calculated as the mean of 12 pre-pandemic samples + 3 SD from Fig. 1.

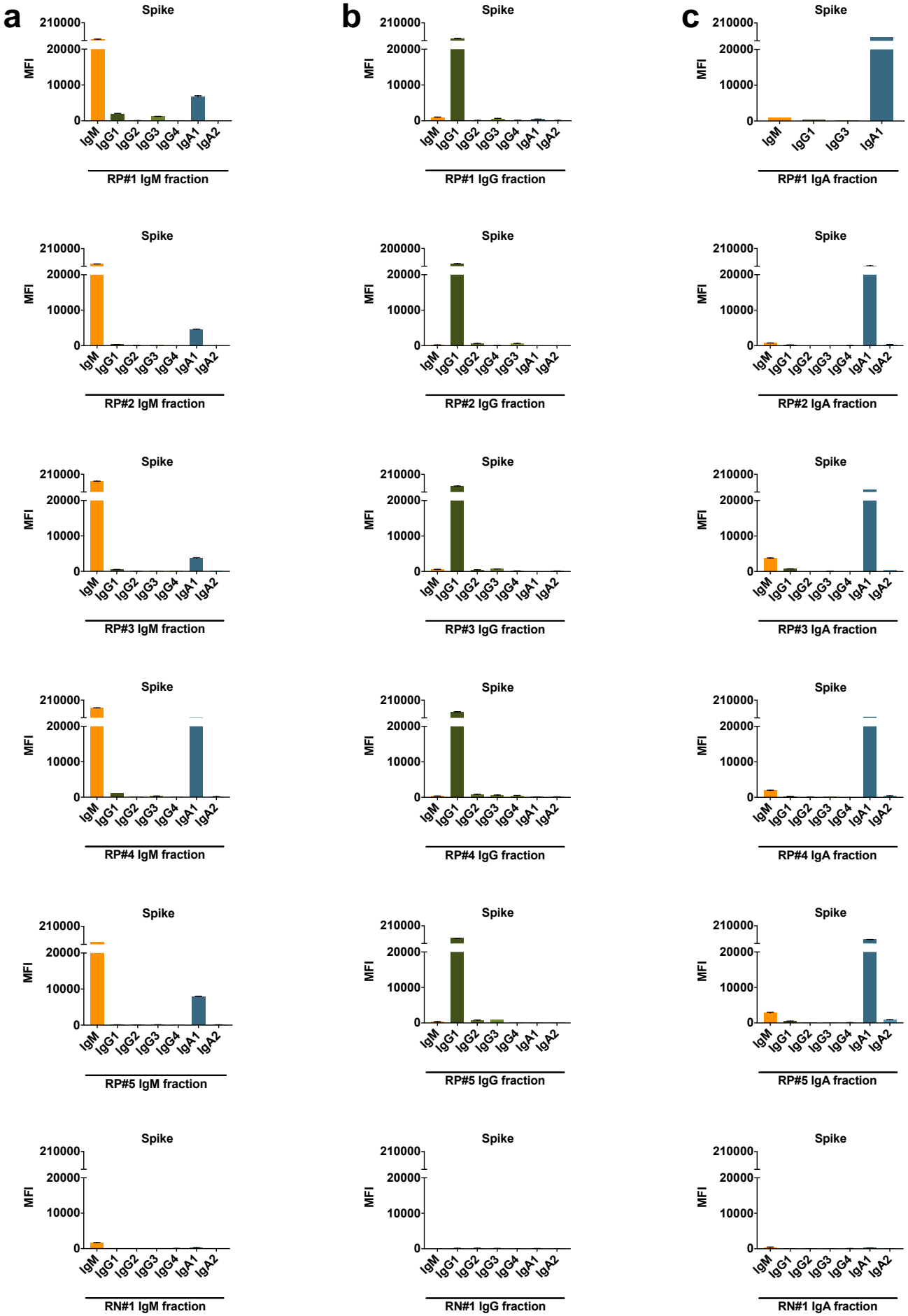
a
b
c
Spike
MFI
210000
20000
10000
0
200000
IgM
IgG1
IgG2
IgG3
IgG4
IgA1
IgA2
RP#1 IgM fraction
RP#1 IgG fraction
RP#1 IgA fraction
RP#2 IgM fraction
RP#2 IgG fraction
RP#2 IgA fraction
RP#3 IgM fraction
RP#3 IgG fraction
RP#3 IgA fraction
RP#4 IgM fraction
RP#4 IgG fraction
RP#4 IgA fraction
RP#5 IgM fraction
RP#5 IgG fraction
RP#5 IgA fraction
RN#1 IgM fraction
RN#1 IgG fraction
RN#1 IgA fraction

Supplementary Fig. 7. Enrichment of spike-specific (a) IgM, (b) IgG, and (c) IgA in purified fractions from RP#1-5 and RN#1. Each fraction was measured for the presence of IgM, IgG1, IgG2, IgG3, IgG4, IgA1, and IgA2 Abs using the isotyping method validated in Supplementary Fig. 3.